

Summation by parts methods for spherical harmonic decompositions of the wave equation in any dimensions

Carsten Gundlach

*School of Mathematics, University of Southampton
Southampton SO17 1BJ, UK
Email: cjg@soton.ac.uk*

José M. Martín-García

*Institut d'Astrophysique de Paris,
CNRS, Univ. Pierre et Marie Curie,
98bis bd Arago, 75014 Paris, France;
Laboratoire Univers et Théories,
CNRS, Univ. Paris Diderot,
5 place Jules Janssen, 92190 Meudon, France
Email: jose@xact.es*

David Garfinkle

*Department of Physics, Oakland University,
Rochester, MI 48309, USA
and Michigan Center for Theoretical Physics,
Randall Laboratory of Physics, University of Michigan,
Ann Arbor, MI 48109-1120, USA
Email: garfinkl@oakland.edu*

We investigate numerical methods for wave equations in $n + 2$ spacetime dimensions, written in spherical coordinates, decomposed in spherical harmonics on S^n , and finite-differenced in the remaining coordinates r and t . Such an approach is useful when the full physical problem has spherical symmetry, for perturbation theory about a spherical background, or in the presence of boundaries with spherical topology. The key numerical difficulty arises from lower-order $1/r$ terms at the origin $r = 0$. As a toy model for this, we consider the flat space linear wave equation in the form $\ddot{\pi} = \psi' + p\psi/r$, $\dot{\psi} = \pi'$, where $p = 2l + n$, and l is the leading spherical harmonic index. We propose a class of summation by parts (SBP) finite differencing methods that conserve a discrete energy up to boundary terms, thus guaranteeing stability and convergence in the energy norm. We explicitly construct SBP schemes that are second and fourth-order accurate at interior points and the symmetry boundary $r = 0$, and first and second-order accurate at the outer boundary $r = R$.

Keywords: Finite differencing, summation by parts, wave equation, spherical harmonics.

CONTENTS

		A. Rigorous treatment of ghost points at $r = 0$	13
I. Introduction	2	B. Solution of the recurrence relations	14
II. Continuum equations and their discretization	3	C. The Evans method	15
A. Continuum equations	3	D. The Sarbach method	16
B. Discretisation	4	E. Continuum boundary conditions involving derivatives	16
C. Summation by parts	4	F. Numerical boundary conditions involving derivatives	17
D. The symmetry boundary $r = 0$	5	G. The projection method for imposing boundary conditions	17
III. Accuracy	5	References	18
A. General considerations	5		
B. Second-order accuracy (SBP2)	6		
C. Fourth-order accuracy (SBP4)	7		
IV. The outer boundary $r = R$	7		
V. Numerical tests	9		
VI. Conclusions	12		
Acknowledgments	13		

I. INTRODUCTION

A standard way of proving that the wave equation on flat spacetime with, for example, Dirichlet boundary conditions is well-posed is to note that it admits an exactly conserved energy. This energy functional can then be used to estimate the solution in terms of the initial and boundary data. The equivalent of well-posedness for the discretised wave equation is called stability. For suitable discretisations, stability can be proved in a discrete energy norm approximating the continuum energy. The Lax equivalence theorem can then be used to prove convergence in the same norm.

When the background spacetime is curved (as in black hole or stellar perturbation theory), and/or when the wave equation acquires lower-order nonlinearities (as in the Einstein equations in generalised harmonic coordinates), it may still be possible to prove well-posedness and stability using the existence of a conserved energy in the constant coefficient approximation to the linearised equation. See [1] for a textbook presentation.

Well-posedness or stability rules out that arbitrarily high frequency perturbations of the solution grow arbitrarily rapidly. Such instabilities in finite difference equations appear in practice as instabilities at the grid frequency that cannot be cured by a small amount of numerical dissipation. They can, however, be efficiently eliminated by making sure that the finite difference scheme conserves a suitable discrete energy when applied to the linear wave equation in flat spacetime. In the context of numerical relativity this was shown in a series of papers [2–4], using finite differencing operators for the wave equation in Cartesian coordinates proposed by Strand [5].

To show that the time derivative of the energy (integrated over space) is given only by boundary terms requires integration by parts. The finite difference operators that preserve a discrete energy up to boundary terms require an equivalent *summation by parts* (from now, SBP) property.

In the interior of the numerical domain, Strand’s SBP operators are just the standard symmetric finite-difference operators of minimal width, for a given order of accuracy. Hence the finite differencing one would naturally use is already SBP except at the boundaries of the numerical domain, and in many numerical relativity applications the outer boundary can be pushed so far out that problems there can be ignored. This makes it easy to overlook the importance of the SBP property for stability. By contrast, [2–4, 6] require full SBP for a clean and stable treatment of inter-block boundaries in multi-block schemes such as the “cubed sphere”.

In this paper we develop SBP methods for the wave equation in *spherical* coordinates. This is natural in three contexts: 1) a spherically symmetric problem; 2) linear perturbations of a spherically symmetric background; 3) a physical domain with a spherical outer boundary. The origin of coordinates then becomes an unphysical interior boundary $r = 0$, which is well-known to cause nu-

merical instabilities, and which is the major obstacle to using spherical coordinates. Our methods remove these instabilities at $r = 0$ completely and provide a stable treatment of the outer boundary $r = R$.

We do not finite-difference in the angles, but rather start by decomposing the solution into spherical harmonics. This is natural for linear equations, where the spherical harmonics decouple, and can be adapted to the non-linear case using pseudo-spectral methods.

After the spherical harmonic decomposition and a reduction to first order (discussed in more detail below) we arrive at the system

$$\dot{\psi} = \pi', \quad \dot{\pi} = \psi' + p\frac{\psi}{r}. \quad (1)$$

where the positive integer p is a combination of the dimension of space and the spherical harmonic index. The finite differencing of these equations, for $p > 0$, is the topic of our paper.

The combination of a spherical harmonic decomposition with finite differencing in r and t of equations of the type (1) has been used in a number of applications: spherical gravitational collapse of a scalar field in higher spacetime dimensions [7, 8], gravitational collapse of a scalar field with angular momentum [9], nonspherical perturbations of spherical relativistic fluid collapse [10] and scalar field collapse [11], general relativistic hydrodynamics [12], and Newtonian magnetohydrodynamics [13–15].

The evolution equations (1) admit the energy

$$E \equiv \frac{1}{2} \int_0^R (\pi^2 + \psi^2), r^p dr \quad (2)$$

with time derivative

$$\frac{dE}{dt} = (r^p \pi \psi)_{r=R}, \quad (3)$$

where Eq. (3) is obtained after using the evolution equations and the identity

$$\int_a^b \left[\left(\psi' + \frac{p}{r} \psi \right) \pi + \pi' \psi \right] r^p dr = [r^p \pi \psi]_a^b \quad (4)$$

[There is no boundary term at $r = 0$ in (3) because ψ vanishes there for regular solutions.] The SBP property that our differential operators need to obey, Eq. (25) below, is the discrete equivalent of (4).

In the linearised Euler equations, for example, (1) is embedded in a larger principal part in such a manner that the identity (4) is still essential for energy conservation. Hence we believe that SBP operators obeying (25) should be used for discretising this piece of the principal part. However, in the present paper we deal explicitly only with the wave equation (1).

Underlining our belief that SBP methods are crucial for stability, the most commonly used second-order accurate discretisation, due to Evans [16], of the spherical wave equation in 3+1 dimensions (the case $p = 2$),

is already SBP in the interior. The SBP approach is *explicitly* used in [17] to produce a second-order accurate implementation of the axisymmetric wave equation (the case $p = 1$, see also the work of Sarbach and collaborators [18] for a generalisation). Unfortunately, neither of these methods seems to admit a generalization to higher than second-order accuracy. Our contribution is to complete the Evans method to make it SBP also at the outer boundary $r = R$, to explicitly construct a fourth-order accurate SBP scheme for any p , and to show how schemes of arbitrary order can be constructed along the same lines.

The plan of the paper is as follows: Sec. 2 presents the continuum wave equation, the equations that come from its expansion in spherical harmonics, and our general SBP discretization framework. Sec. 3 presents our general approach to finding SBP finite difference operators of arbitrary accuracy, with explicit examples given of second-order accurate and fourth-order accurate methods. Sec. 4 treats the outer boundary. Sec. 5 presents numerical tests of our methods and other methods, while conclusions are presented in Sec. 6.

II. CONTINUUM EQUATIONS AND THEIR DISCRETIZATION

A. Continuum equations

In three spatial dimensions, the general solution of the wave equation can be written in a spherical harmonic series as

$$\Phi(r, t, \theta, \varphi) \equiv \sum_{l=0}^{\infty} \sum_{m=-l}^l \phi_{lm}(r, t) Y_{lm}(\theta, \varphi), \quad (5)$$

where the partial waves $\phi_{lm}(r, t)$ obey

$$\ddot{\phi}_{lm} = \phi_{lm}'' + \frac{2}{r} \phi_{lm}' - \frac{l(l+1)}{r^2} \phi_{lm}. \quad (6)$$

A prime denotes $\partial/\partial r$ and a dot $\partial/\partial t$.

This separation of variables ansatz can be generalised to an arbitrary number of space dimensions. In polar coordinates, the Laplace operator Δ in $n+1$ space dimensions can be split into radial and angular derivatives as

$$\Delta = \frac{1}{r^n} \frac{\partial}{\partial r} \left(r^n \frac{\partial}{\partial r} \right) + \frac{1}{r^2} \Delta_{S^n}, \quad (7)$$

where Δ_{S^n} is the Laplace operator on the n -sphere. (For what follows we do not need to introduce coordinates on S^n .) For any integer $n \geq 1$, Δ_{S^n} has eigenfunctions $Y_{l\dots}$ that obey

$$\Delta_{S^n} Y_{l\dots} = -l(l+n-1) Y_{l\dots}, \quad (8)$$

where l takes integer values $l \geq 0$, and the dots stand for $n-1$ further quantum numbers, for example the index

m on Y_{lm} in three spatial dimensions. We can therefore make the separation of variables ansatz

$$\Phi(r, t, \text{angles}) \equiv \sum_{l=0}^{\infty} \sum_{\dots} \phi_{l\dots}(r, t) Y_{l\dots}(\text{angles}) \quad (9)$$

in higher space dimensions, where each partial wave $\phi_{l\dots}$ obeys

$$\ddot{\phi}_{l\dots} = \phi_{l\dots}'' + \frac{n}{r} \phi_{l\dots}' - \frac{l(l+n-1)}{r^2} \phi_{l\dots}. \quad (10)$$

[For $n = 1$, (10) also holds, but l is then the only quantum number, is conventionally called m , and takes both positive and negative integer values.] The restriction to $l = 0$, for any n , gives the spherically symmetric wave equation in $n+1$ space dimensions. From now on, we no longer write the suffix lm or $l\dots$ that labels the spherical harmonic component ϕ .

It appears that we have a family of wave equations in (r, t) parameterised by the two integers n (with $n+1$ the dimension of space) and l (the leading angular quantum number). Considerations of regularity naturally lead us to an alternative form of this wave equation in which those two parameters are merged.

We define Φ to be regular at $r = 0$ if and only if it admits an expansion in positive integer powers of Cartesian coordinates. When Φ is expanded in spherical harmonics as in (9), this criterion holds if and only if

$$\phi(r, t) \equiv r^l \bar{\phi}(r, t), \quad (11)$$

where each $\bar{\phi}$ admits an expansion in positive *even* powers of r . In evolving the wave equation (10), the condition $\phi \sim r^l$ is difficult to enforce numerically except for $l = 0, 1$. It is easier to evolve $\bar{\phi}$ itself with the wave equation

$$\ddot{\bar{\phi}} = \bar{\phi}'' + \frac{p}{r} \bar{\phi}', \quad (12)$$

where

$$p \equiv 2l + n. \quad (13)$$

Recall that $n+1$ is the dimension of space. Hence p is an even integer in an odd number (in particular, three) of space dimensions, and an odd integer in an even number of space dimensions. We stress that in spite of its simple form, this equation represents the wave equation in any number of spatial dimensions in polar coordinates, with or without restriction to $SO(n+1)$ symmetry.

The form (12) of our wave equation can further be reduced to first order in space and time by introducing the auxiliary variables

$$\pi \equiv \dot{\bar{\phi}}, \quad \psi \equiv \bar{\phi}', \quad (14)$$

which obey the system (1) given in the introduction. As $\bar{\phi}$ is an even regular function of r , we have

$$\pi(-r, t) = \pi(r, t), \quad \psi(-r, t) = -\psi(r, t), \quad (15)$$

if we formally extend the functions to negative values of r . Generically, $\bar{\phi} = O(1)$ and hence $\pi = O(1)$ and $\psi = O(r)$ at the origin. Eq. (1) is the form of the wave equation that we will treat for the remainder of the paper, and for which we will find stable and accurate finite difference numerical approximations.

In order to control the growth of E , the boundary term at $r = R$ must be controlled by a suitable boundary condition. Here we consider outer boundary conditions of one of three forms. (For simplicity, we consider only homogeneous boundary conditions.) The well-known maximally dissipative boundary conditions are

$$\rho\pi + \sigma\psi = 0, \quad r = R, \quad \rho\sigma \geq 0. \quad (16)$$

From (3) it is clear that these give $dE/dt \leq 0$. We also consider the higher-order boundary conditions

$$\rho\pi + \mu\pi' = 0, \quad r = R, \quad \rho\mu \geq 0, \quad (17)$$

or

$$\sigma\psi + \nu \left(\psi' + \frac{p}{r}\psi \right) = 0, \quad r = R, \quad \sigma\nu \geq 0. \quad (18)$$

Appendix E shows that these make a modified energy nonincreasing. Hence the wave equation with any of these boundary conditions is well-posed. A continuum energy exists and implies well-posedness also for the more general class of boundary conditions

$$\rho\pi + \sigma\psi + \mu\pi' + \nu(\psi' + p\psi/r) = 0, \quad (19)$$

for certain parameter ranges, but we have not been able to find a discrete counterpart for this case.

B. Discretisation

Throughout this paper we finite-difference in r only, but assume the continuum limit in time. A fully discrete scheme is obtained at the end by using a suitable ODE solver in t (the method of lines).

We use grid functions $\Psi_i(t)$ and $\Pi_i(t)$ on a grid r_i to represent the continuum functions $\pi(r, t)$ and $\psi(r, t)$, assuming that $\Pi_i(t) \equiv \pi(r_i, t)$ and $\Psi_i(t) \equiv \psi(r_i, t)$, and that $\pi(r, t)$ and $\psi(r, t)$ admit Taylor expansions in r to the required order at any r . From now on, we suppress the t -dependence as it is relevant only later when we add time discretisation using the method of lines, that is we write $\pi(r)$ and Π_i , etc. We also use a matrix notation where grid functions are written as column vectors, e.g. Π , and finite differencing operators as matrices acting on these vectors, e.g. $D\Pi$.

A $(2K + 1)$ -point difference operator \tilde{D} is defined by

$$(\tilde{D}\Psi)_i = \sum_{j=i+s-K}^{i+s+K} \tilde{D}_{ij}\Psi_j \quad (20)$$

where $-K \leq s \leq K$ is an offset. The parameters \tilde{D}_{ij} of the difference operator are simply the elements of the band-diagonal matrix \tilde{D} .

We assume a uniform grid with step size $\Delta r \equiv h$. Our methods will require a grid that is either staggered or centred about $r = 0$. In either case we find it convenient to introduce the notation

$$r_i \equiv ih, \quad i = \frac{1}{2}, \frac{3}{2}, \dots, M \quad \text{or} \quad i = 0, 1, \dots, M, \quad (21)$$

that is, the grid index i takes half-integer values for the staggered grid and integer values for the centred grid. In either case $R \equiv r_M \equiv Mh$. Whenever needed, we formally extend the grid functions to any negative value of i with $\Psi_{-i} = -\Psi_i$ and $\Pi_{-i} = \Pi_i$.

C. Summation by parts

As is well-known, the continuum equations (1) are well-posed in the norm provided by E , given in (2) above, because E is conserved. A summation by parts (SBP) finite differencing scheme exactly conserves a discrete equivalent \hat{E} of the continuum energy E . This guarantees that it is stable (the discrete equivalent of well-posed) in the energy norm.

We consider the discrete energy

$$\hat{E} \equiv \frac{1}{2} h^{p+1} \left(\Pi^t W \Pi + \Psi^t \tilde{W} \Psi \right), \quad (22)$$

where t denotes the matrix transpose and where

$$\tilde{W}^t = \tilde{W}, \quad W^t = W, \quad \tilde{W} > 0, \quad W > 0, \quad (23)$$

and we write the finite differencing scheme as

$$\dot{\Psi} = h^{-1} D \Pi, \quad \dot{\Pi} = h^{-1} \tilde{D} \Psi. \quad (24)$$

The powers of h have been introduced so that $W, \tilde{W}, D, \tilde{D}$ are all dimensionless and independent of h . The quantity $r_i/h = i$ also has this property. We will derive explicit expressions later, but both $h^p W$ and $h^p \tilde{W}$ approximate r^p , while $h^{-1} D$ approximates d/dr and $h^{-1} \tilde{D}$ approximates $d/dr + p/r$.

The SBP property that guarantees that \hat{E} is constant up to boundary terms is

$$W \tilde{D} + (\tilde{W} D)^t = B, \quad (25)$$

where the boundary operator B is defined by

$$\Pi^t B \Psi \equiv \chi M^p \Pi_M \Psi_M, \quad (26)$$

and the constant χ obeys $\chi \rightarrow 1$ in the continuum limit $M \rightarrow \infty$ as $h \rightarrow 0$ at fixed $r = R$. [There is no boundary contribution at $r = 0$, consistent with the fact that we impose $\psi(0) = 0$.] Eq. (25) is the discrete equivalent of (4).

As W is positive definite, it is invertible, and we can consider \tilde{D} as determined by a choice of D, W, \tilde{W} and B :

$$\tilde{D} = -W^{-1} D^t \tilde{W} + W^{-1} B. \quad (27)$$

In the case $p = 0$ considered by Strand [5], W and \tilde{W} represent 1, and \tilde{D} and D both represent d/dr . It is then natural to set $W = \tilde{W}$ and $D = \tilde{D}$.

D. The symmetry boundary $r = 0$

In numerical simulations using polar coordinates one is faced with the fact that $r = 0$ is a boundary of the numerical grid, but is not in fact a boundary of the physical domain. As a result, there are (typically) no physical boundary conditions one can or must impose in the continuum limit, but the numerical simulation does require boundary conditions. These are derived from the assumption that the desired solution is not less differentiable at $r = 0$ than for $r > 0$. As stated earlier, we assume Φ to be smooth in Cartesian spatial coordinates, which is equivalent to π being smooth and even and ψ being smooth and odd. The standard general approach to imposing such “symmetry boundary conditions” or “regularity conditions” is to extend the numerical grid into a small number of “ghost points” representing negative r which are populated by the assumed even or odd parity of the grid functions. Standard centred finite differencing methods can then be used at and near the boundary as if it was an interior point.

From a strict SBP point of view, there are no ghost points, and finite difference operators are necessarily skewed near the boundary. The fact that $r = 0$ is not a physical boundary is represented by the fact that B is zero at the boundary $r = 0$.

However, we find that the use of ghost points as a notational device allows a simpler derivation, presentation, and application of our results, in that we do not need to discuss $r = 0$ explicitly as a boundary. Rather than introduce a few ghostpoints, for our *derivation* we extend all grid objects from $1/2$ or $0, \dots, M$ to $-M, \dots, M$, corresponding to $-R \leq r \leq R$. We can then formally treat $r = 0$ as an interior point.

We extend the grid functions to negative i as

$$\Pi_{-i} = \Pi_i, \quad \Psi_{-i} = -\Psi_i. \quad (28)$$

Because W and \tilde{W} are used only to define \hat{E} , we can assume without loss of generality that

$$W_{-i,-j} \equiv W_{ij}, \quad W_{-i,j} \equiv W_{i,-j} = 0, \quad i, j > 0, \quad (29)$$

and similarly for \tilde{W} . B is extended by $B_{-M,-M} = -B_{MM}$. In Appendix A we prove from these assumptions that (28) holds at all times if and only if

$$D_{-i,-j} = -D_{ij}. \quad (30)$$

When *coding* our method, we implement D and \tilde{D} with a few ghost points. Equivalently, the ghost points can be explicitly eliminated. A rigorous discussion of this point is relegated to Appendix A, as it introduces additional notation not required for our main argument. Obviously, our time updates will by construction exactly preserve the evenness of π and oddness of ψ .

III. ACCURACY

A. General considerations

In this section, we will consider only the behavior of the finite difference operators at interior points (including $r = 0$) of the numerical grid, postponing to the next section the discussion of how the operators behave at and near the outer boundary. In what follows, we will always choose the finite difference operator D to be a standard centred difference operator of the appropriate order. That is, for second-order accurate methods, for interior points, we will choose

$$(D\Pi)_i \equiv \frac{\Pi_{i+1} - \Pi_{i-1}}{2}, \quad (31)$$

while for fourth-order accurate methods, we will choose

$$(D\Pi)_i \equiv \frac{8(\Pi_{i+1} - \Pi_{i-1}) - (\Pi_{i+2} - \Pi_{i-2})}{12}. \quad (32)$$

Once we choose W and \tilde{W} , the operator \tilde{D} is given by Eq. (27) and the scheme preserves the discrete energy of Eq. (22), and thus is stable. Our task then is to choose W and \tilde{W} in such a way that the operator $h^{-1}\tilde{D}$ so determined is an accurate (to the chosen order) finite difference representation of the continuum operator $d/dr + p/r$.

In analyzing the accuracy of \tilde{D} it is helpful to write the grid values $\Psi_j = \psi(r_j)$ in terms of the Taylor expansion of $\psi(r)$ about the fixed grid point r_i . We can then write

$$h^{-1}(\tilde{D}\Psi)_i = c_{0i}h^{-1}\psi(r_i) + c_{1i}\psi'(r_i) + c_{2i}h\psi''(r_i) + \dots + h^{2K-1}c_{2K,i}\psi^{(2K)}(r_i) + O(h^{2K}), \quad (33)$$

where the $c_{\alpha i}$ are a set of numbers linearly related in a straightforward way to the \tilde{D}_{ij} at each point i . In the following we adopt a simplified notation where the $c_{\alpha i}$ (with $\alpha = 0, \dots, 2K$) are written as c_α , $\psi(r_i)$ simply as ψ , etc., and r_i simply as r . That is, we do not write the dependence on i , and all continuum quantities are evaluated at $r = r_i$.

The difference operator \tilde{D} is said to be accurate to order $2N$ if it obeys (using our abbreviated notation)

$$h^{-1}(\tilde{D}\Psi)_i = \frac{p}{r}\psi + \psi' + O(h^{2N}). \quad (34)$$

The point at $r = 0$, which arises (only) on a centred grid, must be treated specially. Taking the limit as $r \rightarrow 0$ of Eq. (34) at finite h we see that at $r = 0$

$$c_1 = 1 + p \quad (35)$$

while the other odd c_α vanish and the even c_α are undetermined.

A key observation for what follows is that (34) needs to be obtained formally in the limit $h \rightarrow 0$, *both* at (approximately) constant r , and at constant i . The possible problem with the latter limit are error terms of the

form h^m/r^n , which are $O(h^m)$ at constant r , but only $O(h^{m-n})$ at constant i .

Naively one would expect the accuracy requirement (34) for \tilde{D} at $r \neq 0$ to be equivalent to the following constraints on the coefficients of the difference operator (as defined above):

$$c_0 = \frac{ph}{r}, \quad c_1 = 1, \quad c_2 = \dots = c_{2N} = 0. \quad (36)$$

Clearly, we would need a stencil of width $2N+1$ or larger to control all these c_α , as, for $p > 0$, the even c_α cannot be set to zero just by using a symmetric stencil. However, we shall now see that we can violate some of the equalities (36) as $r \rightarrow 0$ and in effect replace them with approximate equalities. The effect is that we will only need an $N+1$ point stencil.

Rather than devising a general notation, we present the cases $N=1$ and $N=2$, after which it should be clear how one can proceed to arbitrary N .

For $N=1$, we make the following ansatz:

$$c_0 = \frac{ph}{r} + \delta_0 \left(\frac{h}{r}\right)^3, \quad (37)$$

$$c_1 = 1 - \delta_0 \left(\frac{h}{r}\right)^2, \quad (38)$$

$$c_2 = \delta_1 \left(\frac{h}{r}\right), \quad (39)$$

where the δ_α may depend on i . The special case $\delta_0 = \delta_1 = 0$ brings us back to (36), but we shall now see that the parameters δ_α do not need to vanish identically but only need to be bounded because of the way ψ' approximates ψ/r and vice versa for regular odd functions $\psi(r)$ as $r \rightarrow 0$. Substituting this ansatz into (33) gives

$$h^{-1}(\tilde{D}\Psi)_i = \frac{p}{r}\psi + \psi' + \delta_0 h^2 \left[r^{-2} \left(\frac{\psi}{r} - \psi' \right) \right] + \delta_1 h^2 [r^{-1}\psi''] + R_2. \quad (40)$$

Here

$$R_2 = c_3 h^2 \psi''' + c_4 h^3 \psi'''' + \dots, \quad (41)$$

where for a 3-point stencil c_3, c_4, \dots are known linear functions of c_0, c_1 and c_2 . Now, because ψ can be expanded in positive odd integer powers of r , both square brackets in (40) are actually $O(1)$ as $r \rightarrow 0$. Therefore, as long as δ_0 and δ_1 are bounded uniformly in i , the coefficients of h^2 in (40) are bounded uniformly in i . Similarly, as c_3, c_4, \dots are regular functions of δ_0 and δ_1 , the coefficients of h^2 and all higher powers of h in (41) are also explicitly regular at $r=0$ and so we have the desired second-order accuracy, uniformly in i .

For $N=2$ we make the ansatz

$$c_0 = \frac{ph}{r} + \delta_0 \left(\frac{h}{r}\right)^5, \quad (42)$$

$$c_1 = 1 - \delta_0 \left(\frac{h}{r}\right)^4, \quad (43)$$

$$c_2 = \left(\frac{\delta_0}{3} + \delta_1\right) \left(\frac{h}{r}\right)^3, \quad (44)$$

$$c_3 = -\delta_1 \left(\frac{h}{r}\right)^2, \quad (45)$$

$$c_4 = \delta_2 \left(\frac{h}{r}\right), \quad (46)$$

which gives

$$h^{-1}(\tilde{D}\Psi)_i = \frac{p}{r}\psi + \psi' + \delta_0 h^4 \left[r^{-3} \left(\frac{\psi}{r^2} - \frac{\psi'}{r} + \frac{\psi''}{3} \right) \right] + \delta_1 h^4 \left[r^{-2} \left(\frac{\psi''}{r} - \psi''' \right) \right] + \delta_2 h^4 [r^{-1}\psi''''] + R_4, \quad (47)$$

where $R_4 = O(h^4)$ in the sense discussed above. Again, all the square brackets are regular at $r=0$, and so we have fourth-order accuracy if and only if the $\delta_{\alpha i}$ are bounded uniformly in i .

It should now be clear that this method can be extended to arbitrary N , giving N equations to be solved through a suitable choice of W and \tilde{W} , and $N+1$ inequalities (uniform in i bounds on the $\delta_{\alpha i}$) to be then verified for that solution.

Informally, our method can be described as “trading r for h ”. It works because the terms in square brackets above are all $O(1)$ as $r \rightarrow 0$, which in turn requires $\psi(r)$ to be a regular odd function of r .

Our task has thus become to choose W and \tilde{W} in such a way that the operator \tilde{D} given by equation (27) satisfies our ansatz [Eqs. (37-39) for $N=1$ and Eqs. (42-46) for $N=2$] such that the quantities δ_α are uniformly bounded. We now show explicitly how this task can be accomplished.

B. Second-order accuracy (SBP2)

We begin with the case $N=1$. For simplicity, we choose W and \tilde{W} to be diagonal. That is,

$$W = \text{diag}(w_i), \quad \tilde{W} = \text{diag}(v_i). \quad (48)$$

The SBP formula (27) then gives

$$(\tilde{D}\Psi)_i = \frac{v_{i+1}\Psi_{i+1} - v_{i-1}\Psi_{i-1}}{2w_i} \quad (49)$$

for interior points.

We have allowed for $v_i \neq w_i$ because this allows us to cover the Evans and Sarbach methods reviewed in the Appendix, but for the remainder of this Subsection we further restrict our ansatz to $v_i = w_i$, using w_i as the parameters. We can then read off c_0, c_1 and c_2 in terms of w_i . The one equality contained in (37-39), namely

$$\left(\frac{r}{h}\right) c_0 + c_1 = 1 + p, \quad (50)$$

keeping in mind that $r/h = i$, gives a linear recurrence relation of degree 2 for w_i ,

$$(i+1)w_{i+1} - (i-1)w_{i-1} = 2(p+1)w_i. \quad (51)$$

The other two accuracy conditions define δ_1 and δ_2 in terms of w_i . On a *staggered* grid, from (29) we have $w_{-1/2} = w_{1/2}$. We initially fix an arbitrary value for $w_{1/2}$, and can then solve the recursion for w_i for all $i \geq 3/2$. (Note that \tilde{D} is unchanged if W and \tilde{W} are multiplied by the same constant factor). On a *centred grid*, evaluating Eq. (35) with $w_{-1} = w_1$ gives $w_1 = (1+p)w_0$. We initially fix an arbitrary value of w_0 and can then solve the recursion for w_i for all $i \geq 2$.

The w_i determine the operator \tilde{D} which in turn determines the quantities δ_0 and δ_1 . These quantities are plotted in Fig. 8. Note that these quantities are uniformly bounded, which confirms that our method is second-order accurate. Appendix B confirms this analytically. For comparison, Fig. 8 also contains the corresponding quantities for the method of Evans [16], which we present in our notation in Appendix C.

C. Fourth-order accuracy (SBP4)

We now turn to the case of $N = 2$, that is a fourth-order accurate scheme. We can no longer choose W and \tilde{W} to be identical and diagonal. Instead, we choose W to be diagonal and \tilde{W} to be band-diagonal with three bands. We parameterize them as

$$W_{i,i} = w_i, \quad w_{-i} = w_i, \quad (52)$$

$$\tilde{W}_{i,i} = v_i, \quad v_{-i} = v_i, \quad (53)$$

$$\tilde{W}_{i,i+1} = u_{i+1/2}, \quad u_{-i} = u_i, \quad (54)$$

$$\tilde{W}_{i,i-1} = u_{i-1/2}, \quad (55)$$

and all other components zero, where on the staggered grid the index on v and w takes half-integer values and the index on u takes integer values, and the other way around on the centred grid. In the interest of simplicity, we would like to have as few nonvanishing u_i as possible. On the staggered grid it is possible to have only u_1 nonvanishing, while on the centred grid, it is possible to make only $u_{3/2}$ and $u_{5/2}$ nonvanishing. From now on, we make this choice of u_i .

The ansatz of Eqs. (42-46) imply two equalities, namely Eq. (50) and

$$c_1 + 3\frac{h}{r}c_2 + 3\left(\frac{h}{r}\right)^2 c_3 = 1. \quad (56)$$

If we temporarily take u_i as given, Eqs. (50) and (56) determine the w_i plus a linear recurrence relation of order 4 for the v_i . On the *staggered* grid, we can fix $v_{1/2} = v_{-1/2}$ and $v_{3/2} = v_{-3/2}$ arbitrarily, and solve the recurrence relation for v_i for $i \geq 5/2$ starting from

those four points and our choice of u_1 . On the *centred* grid, the accuracy conditions (35) at the origin reduce to $(1+p)w_0 = v_1 - (1/8)u_{3/2} + (5/8)u_{5/2}$ and $v_2 = v_1 + (63/8)u_{3/2} - (27/8)u_{5/2}$. We can fix v_1 and choose $u_{3/2}$ and $u_{5/2}$ arbitrarily and then compute v_i for $i \geq 3$ from the recurrence relation. (Note that v_0 multiplies Ψ_0 , which vanishes, and hence does not participate in the recurrence.) It remains to fix the u_i . Appendix B shows in detail how they are uniquely determined by the requirement that v_i and w_i approximate i^p as $i \rightarrow \infty$.

Having found the u_i , v_i and w_i , the operator \tilde{D} is given by

$$(\tilde{D}\Psi)_i = \frac{8(\tilde{\Psi}_{i+1} - \tilde{\Psi}_{i-1}) - (\tilde{\Psi}_{i+2} - \tilde{\Psi}_{i-2})}{12w_i}, \quad (57)$$

where we have introduced the shorthand

$$\tilde{\Psi}_{1/2} \equiv v_{1/2}\Psi_{1/2} + u_1\Psi_{3/2}, \quad (58)$$

$$\tilde{\Psi}_{3/2} \equiv v_{3/2}\Psi_{3/2} + u_1\Psi_{1/2}, \quad (59)$$

$$\tilde{\Psi}_i \equiv v_i\Psi_i, \quad i \geq 5/2. \quad (60)$$

for the staggered grid and

$$\tilde{\Psi}_0 \equiv 0, \quad (61)$$

$$\tilde{\Psi}_1 \equiv v_1\Psi_1 + u_{3/2}\Psi_2, \quad (62)$$

$$\tilde{\Psi}_2 \equiv v_2\Psi_2 + u_{3/2}\Psi_1 + u_{5/2}\Psi_3, \quad (63)$$

$$\tilde{\Psi}_3 \equiv v_3\Psi_3 + u_{5/2}\Psi_2, \quad (64)$$

$$\tilde{\Psi}_i \equiv v_i\Psi_i, \quad i \geq 4. \quad (65)$$

for the centred grid.

The δ_i of this method are plotted in Fig. 9. These δ_i are uniformly bounded, which demonstrates that this method is fourth-order accurate.

IV. THE OUTER BOUNDARY $r = R$

We begin by recalling Strand's method [5] for treating the wave equation including boundaries. The one-dimensional wave equation in first order form is

$$\dot{\pi} = \psi', \quad \dot{\psi} = \pi', \quad a \leq x \leq b \quad (66)$$

with energy

$$E = \int_a^b (\pi^2 + \psi^2) dx, \quad \frac{dE}{dt} = [\pi\psi]_a^b. \quad (67)$$

It is natural to discretize this symmetrically in π and ψ , that is

$$\dot{\Pi} = D_0\Psi, \quad \dot{\Psi} = D_0\Pi, \quad (68)$$

with energy

$$\hat{E} = \frac{h}{2} (\Pi^t W_0 \Pi + \Psi^t W_0 \Psi). \quad (69)$$

and SBP condition

$$W_0 D_0 + (W_0 D_0)^t = B_0, \quad (70)$$

with $B_0 = \text{diag}(1, 0, \dots, 0, 1)$, as there are two boundaries. Note that this problem is translation-invariant in the interior, and so D_0 and W_0 will naturally be translation-invariant in the interior, except for finite-sized end blocks. D_0 and W_0 with various orders of accuracy in the interior and at the boundaries have been constructed by Strand [5]. (We have added the suffix 0 to indicate that this is the special case $p = 0$ of our problem.)

In (1) with $p > 0$ additional problems result because the equations are not translation-invariant but depend explicitly on r . In previous Sections we have addressed these problems at interior points and at the pseudo-boundary $r = 0$.

Strand provides a class of norms W_0 that are unit diagonal except near the boundaries, as well as compatible derivative operators D_0 that are the standard minimal width centred difference operators, except near the boundaries. Hence D_0 agrees with our D except at the outer boundary. Let W_∞ and \tilde{W}_∞ denote our previously derived weights for the problem on $0 \leq r < \infty$, and simply truncated to the range $i = -M, \dots, M$. We now define operators with a boundary at $i = \pm M$, corresponding to $r = \pm R$, as follows:

$$W := W_0 W_\infty, \quad (71)$$

$$\tilde{W} := \tilde{W}_0 W_\infty, \quad (72)$$

$$D := D_0, \quad (73)$$

$$\tilde{D} := W^{-1} D_0 \tilde{W}. \quad (74)$$

It is now straightforward to verify that the operators and weights thus defined obey the desired SBP property (25) with boundary operator

$$B = B_0 \tilde{W}_\infty, \quad (75)$$

using (70). It is essential in this calculation that \tilde{W}_∞ and W_0 commute. This is true because \tilde{W}_∞ is diagonal except near the origin, and W_0 is diagonal everywhere and unit diagonal except near the outer boundary.

The D and \tilde{D} thus defined agree with their previously constructed infinitely extended versions except near the boundary, and so we need to establish their accuracy only

near the boundary. By Strand's construction, using relaxed notation,

$$h^{-1} D_0 = \frac{d}{dr} + O(h^{-\tau}) \quad (76)$$

near the boundary. Also by construction,

$$h^p W_\infty = r^p + O(h^{-2N}), \quad h^p \tilde{W}_\infty = r^p + O(h^{-2N}), \quad (77)$$

near the boundary, with $2N \geq \tau$, and similarly for \tilde{W}_∞ . Substituting these into (74), we find

$$h^{-1} \tilde{D} = \frac{d}{dr} + \frac{p}{r} + O(h^{-\tau}). \quad (78)$$

Hence D and \tilde{D} have the same accuracy both in the interior and at the boundary, and the same stencil, as the minimal width SBP operator with diagonal norm D_0 of Strand. In this sense, they are optimal.

Applying the general prescription above to our second-order accurate method SBP2 or to the second-order accurate Evans and Sarbach methods reviewed in the Appendix, we have

$$D = \begin{pmatrix} \cdot & & & & \\ & \cdot & & & \\ & -\frac{1}{2} & 0 & \frac{1}{2} & \\ & & -\frac{1}{2} & 0 & \frac{1}{2} \\ & & & -1 & 1 \end{pmatrix}, \quad (79)$$

$$\tilde{D} = \begin{pmatrix} \cdot & & & & \\ & \cdot & & & \\ & -\frac{v_{M-3}}{2w_{M-2}} & 0 & \frac{v_{M-1}}{2w_{M-2}} & \\ & & -\frac{v_{M-2}}{2w_{M-1}} & 0 & \frac{v_M}{2w_{M-1}} \\ & & & -\frac{v_{M-1}}{w_M} & \frac{v_M}{w_M} \end{pmatrix}, \quad (80)$$

$$W = \text{diag} \left(\dots, w_{M-2}, w_{M-1}, \frac{w_M}{2} \right), \quad (81)$$

$$\tilde{W} = \text{diag} \left(\dots, v_{M-2}, v_{M-1}, \frac{v_M}{2} \right), \quad (82)$$

$$B = \text{diag} (\dots, 0, 0, v_M). \quad (83)$$

As an example of the general result (78), we have

$$\begin{aligned} (\tilde{D}\Psi)_M &= -\frac{v_{M-1}}{w_M} \psi_{M-1} + \frac{v_M}{w_M} \psi_M \\ &= \frac{v_M - v_{M-1}}{w_M} \psi(R) + \frac{v_{M-1}}{w_M} h \psi'(R) + O(h^2) \\ &= h \left[\psi'(R) + \frac{p}{R} \psi(R) + O(h) \right], \end{aligned} \quad (84)$$

Hence this method is first-order accurate at the boundary point $i = M$. The above expressions hold for the Evans, Sarbach and SBP2 methods with the appropriate v_i and w_i . In the last two of these, $v_i = w_i$.

Applying our general outer boundary prescription to our fourth-order accurate method SBP4, we can impose

accuracy at the boundary of order $\tau = 1$ or $\tau = 2$. For $\tau = 1$, following the general prescription given above, we set

$$D = \begin{pmatrix} \cdot & & & & \\ \frac{1}{12} & -\frac{2}{3} & 0 & \frac{2}{3} & -\frac{1}{12} \\ & \frac{1}{13} & -\frac{8}{13} & 0 & \frac{7}{13} \\ & & \frac{1}{5} & -\frac{7}{5} & \frac{6}{5} \\ & & & & \end{pmatrix}, \quad (85)$$

$$\tilde{D} = \begin{pmatrix} \cdot & & & & \\ \frac{v_{M-4}}{12w_{M-2}} & -\frac{2v_{M-3}}{3w_{M-2}} & 0 & \frac{2v_{M-1}}{3w_{M-2}} & -\frac{v_M}{12w_{M-2}} \\ & \frac{v_{M-3}}{13w_{M-1}} & -\frac{8v_{M-2}}{13w_{M-1}} & 0 & \frac{7v_M}{13w_{M-1}} \\ & & \frac{v_{M-2}}{5w_M} & -\frac{7v_{M-1}}{5w_M} & \frac{6v_M}{5w_M} \\ & & & & \end{pmatrix}, \quad (86)$$

$$W = \text{diag} \left(\dots, w_{M-2}, \frac{13w_{M-1}}{12}, \frac{5w_M}{12} \right), \quad (87)$$

$$\tilde{W} = \text{diag} \left(\dots, v_{M-2}, \frac{13v_{M-1}}{12}, \frac{5v_M}{12} \right), \quad (88)$$

$$B = \text{diag} (\dots, 0, 0, v_M). \quad (89)$$

For $\tau = 2$, following the general prescription we set

$$\tilde{D} = \begin{pmatrix} \cdot & & & & & & \\ \frac{v_{M-6}}{12w_{M-4}} & -\frac{2v_{M-5}}{3w_{M-4}} & 0 & \frac{2v_{M-3}}{3w_{M-4}} & -\frac{v_{M-2}}{12w_{M-4}} & 0 & 0 \\ 0 & \frac{4v_{M-5}}{49w_{M-3}} & -\frac{32v_{M-4}}{49w_{M-3}} & 0 & \frac{59v_{M-2}}{98w_{M-3}} & 0 & -\frac{3v_M}{98w_{M-3}} \\ 0 & 0 & \frac{4v_{M-4}}{43w_{M-2}} & -\frac{59v_{M-3}}{86w_{M-2}} & 0 & \frac{59v_{M-1}}{86w_{M-2}} & -\frac{4v_M}{43w_{M-2}} \\ 0 & 0 & 0 & 0 & -\frac{v_{M-2}}{2w_{M-1}} & 0 & \frac{v_M}{2w_{M-1}} \\ 0 & 0 & 0 & \frac{3v_{M-3}}{34w_M} & \frac{4v_{M-2}}{17w_M} & -\frac{59v_{M-1}}{34w_M} & \frac{24v_M}{17w_M} \end{pmatrix}, \quad (90)$$

$$W = \text{diag} \left(\dots, w_{M-4}, \frac{49w_{M-3}}{48}, \frac{43w_{M-2}}{48}, \frac{59w_{M-1}}{48}, \frac{17w_M}{48} \right), \quad (91)$$

$$\tilde{W} = \text{diag} \left(\dots, v_{M-4}, \frac{49v_{M-3}}{48}, \frac{43v_{M-2}}{48}, \frac{59v_{M-1}}{48}, \frac{17v_M}{48} \right), \quad (92)$$

$$B = \text{diag} (\dots, 0, 0, v_M). \quad (93)$$

The expression for D is obtained by setting v_i and w_i to 1 in \tilde{D} . We shall call our SBP4 method with $\tau = 1, 2$ SBP41 and SBP42 respectively.

V. NUMERICAL TESTS

We have implemented our SBP2, SBP41 and SBP42 methods described above, combined with fourth-order Runge-Kutta (RK4) discretisation in time. For comparison, we have also implemented the Evans method (turned into an SBP method by the boundary treatment of Sec. IV) and the Sarbach method. To complete the numerical setup, we need to choose continuum boundary conditions at the physical outer boundary $r = R$ and a way of enforcing them. For our tests, we choose either homogenous maximally dissipative boundary or the derivative boundary conditions derived in Appendixes E

and F, and implement them using the Olsson projection method [19], which for completeness we review in Appendix G.

In SBP4 we use the numerical coefficients \tilde{D}_{ij} , or equivalently u_i , \bar{v}_i and \bar{w}_i , calculated by the relaxation method described in Appendix B up to $i \sim 2000$, and using the asymptotic results (B14), (B15) for larger i .

For all evolutions shown here, we use initial data

$$\psi(r, 0) = 0, \quad \pi(r, 0) = e^{-\frac{(r-r_0)^2}{d^2}} + e^{-\frac{(r+r_0)^2}{d^2}} \quad (94)$$

with $r_0 = 5$ and $d = 2$. (The Gaussian at negative r is needed to make $\pi(r)$ strictly even.) The numerical domain is $0 \leq r \leq R$ with $R = 25$. This means that the wave is initially well separated from both boundaries, and interacts with the symmetry boundary around $t \sim 5$ and with the outer boundary around $t \sim 20$. We continue the evolution until $t = 40$.

By construction, all our SBP methods are stable in the

energy norm and consistent with the continuum equations. From the Lax equivalence theorem we therefore expect convergence to the continuum in the energy norm E , or in other words we expect convergence of $r^{p/2}\pi$ and $r^{p/2}\psi$ in the uniform L^2 norm. We verify this expectation, but beyond that we also look for pointwise convergence of these variables.

To check convergence, on a centred grid we compare evolutions at five grid resolutions, from $h = 1/10$ down to $2^{-4} \cdot 1/10$, each to a reference evolution at $h = 2^{-7} \cdot 1/10$. (By comparison, using refinement by a factor of 3 on the *staggered* grid allows us to fix $r_M = R$, and while appropriate points of all refined grids still align with the coarsest grid. Keeping R exactly resolution-independent is essential for comparing different resolutions, while aligned grids avoid the need for interpolation.) We use a Courant factor $\Delta t/h = 1/4$ throughout. We plot

$$e_{\pi,k}(r, t; h) \equiv \left(\frac{h}{1/10}\right)^{-k} r^{p/2} [\pi(r, t; h) - \pi(r, t; h_{\text{ref}})] \quad (95)$$

and its norm

$$|e_{\pi,k}(\cdot, t; h)| \equiv \left(\frac{1}{R} \int_0^R e_{\pi,k}(r, t; h)^2 dr\right)^{1/2}, \quad (96)$$

and similarly for the variable ψ . For h small enough, where a Richardson expansion of the error holds and is dominated by the leading $O(h^k)$ term, $e_{\pi,k}$ and its norm should be approximately independent of h (with the differences generated by subdominant error terms).

We have tested the Evans, Sarbach, SBP2, SBP41 and SBP42 methods with a selection of outer boundary conditions and with p in the range $1 \leq p \leq 22$. Note however the following exceptions: 1. the Evans method is not defined on the staggered grid for odd p ; 2. the Sarbach method is only defined on the centred grid; 3. for $p = 1$ Evans, Sarbach and SBP2 on a centred grid are identical. We now summarise our results. In all evolutions shown in the following *figures*, we set $p = 6$ (corresponding to $l = 2$ spherical harmonics in 3 space dimensions), use a grid centred on $r = 0$, and the boundary condition $\pi = 0$.

The three 2nd-order accurate methods, SBP2, Sarbach and Evans all show 2nd-order pointwise convergence (and hence also convergence in the energy norm) throughout the evolution. Fig. 1 demonstrates 2nd-order convergence in the energy norm for SBP2, for all t , while Fig. 2 demonstrates pointwise convergence at $t = 14.25$. The error e_2 is almost identical for all methods. Until the wave has interacted with the outer boundary, it appears smooth, while afterwards there is a small admixture of an oscillation with the grid frequency.

For our 4th-order accurate method with 1st and 2nd-order accurate boundary conditions, SBP41 and SBP42, we see 4th-order pointwise (and hence energy norm) convergence until the wave interacts with the outer boundary. Fig. 3 demonstrates this for SBP41. After the wave has interacted with the boundary, SBP41 drops to

2nd-order convergence in the energy norm (see Fig. 4), while SBP42 drops to 3rd-order convergence in the energy norm (see Fig. 5). Note that in each case the global accuracy is one order higher than the accuracy τ of D and \tilde{D} at the boundary. For both methods, the error after the interaction with the boundary is dominated by an oscillation with the grid frequency, with a smooth envelope, and so they do not converge pointwise in the standard sense, although the envelope of the grid frequency noise does. Fig. 6 is a snapshot that shows the transition from 4th-order pointwise convergence to this behaviour as the wave begins to interact with the boundary.

Two comments on our convergence tests are worth making: First, note that the Lax theorem only gives convergence in L^2 of $r^{p/2}\pi$, $r^{p/2}\psi$. We do find this in our tests, but we also find pointwise convergence at the same rates, at all times for SBP2, and for SBP4 before the wave interacts with the outer boundary. One can go further and look at the convergence of the unscaled variables π , ψ , for which the theory makes no prediction. We find that they converge pointwise for $p \lesssim 4$ at all times, and for all p while the wave is away from the symmetry boundary. However, while the wave is reflected at the origin, the continuum solution oscillates rapidly approximately p times. (This can be shown by constructing the exact solution as a sum involving the first p derivatives of the initial data.) A small phase error at this stage gives rise to a very large pointwise error and pointwise convergence is lost (at the resolutions we ran). However, as the solution moves out again, different resolutions agree again much better. This is compatible with the observed pointwise convergence of $r^{p/2}\pi$, $r^{p/2}\psi$ because in these rescaled variables the complicated continuum behaviour at the origin is hidden and so is the momentary increase of the error.

Our second comment is that the general theory for the accuracy of first-order hyperbolic initial-boundary value problems [1, 20–22] suggests that the order of global accuracy is determined by the lower of the order of the physical boundary conditions, and the order of purely numerical (“extra”) boundary conditions plus 1. In our case we always have one physical and one extra boundary condition. The accuracy order of the physical boundary condition is ∞ for maximally dissipative physical boundary conditions ($\mu = \nu = 0$) and τ for physical boundary conditions involving a derivative (μ or $\nu \neq 0$), as we discretise these using D and \tilde{D} on the boundary. The accuracy order of the extra boundary condition is always τ , as it relies on evaluating D and \tilde{D} on the boundary. Hence we would expect global accuracy of order $\tau + 1$ for any maximally dissipative boundary condition, and τ for any boundary condition involving a derivative. However, experimentally we find $\tau + 1$ in both cases, which means that the maximally dissipative boundary conditions perform as expected, and the derivative boundary conditions perform one order better than expected. The latter point is illustrated in Fig. 7.

As a further test of the predicted behaviour of our

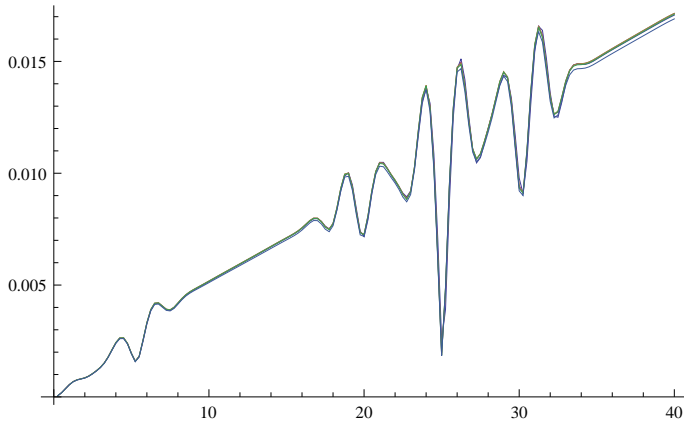


FIG. 1. 2nd-order convergence in the energy norm of SBP2 for $p = 6$, with the initial data given in the text. We show $|e_{\pi,2}(\cdot, t; h)|$ against t at 5 different resolutions with h decreasing by factors of 2 from $1/10$ to $1/160$. The 5 curves are on top of each other, demonstrating 2nd-order convergence. With the normalisation of Eq. (96), they indicate the actual L^2 numerical error at resolution $h = 1/10$ (meaning there are ~ 40 gridpoints across the wave packet). The equivalent curves for ψ and for the Sarbach and Evans numerical methods are similar.

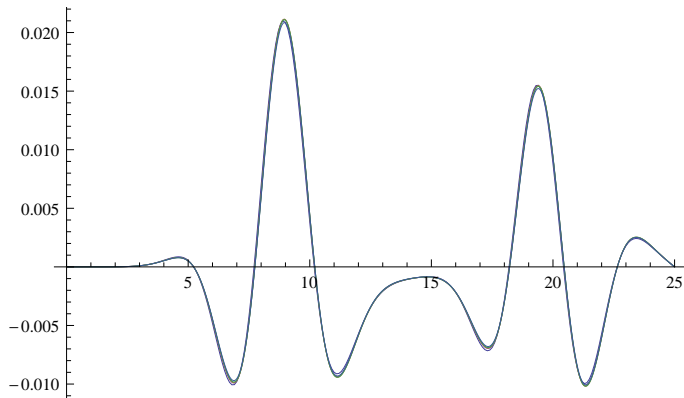


FIG. 2. 2nd-order pointwise convergence of the same evolution. We show $e_{\pi,2}(r, t; h)$ at $t = 14.25$ against r . The 5 curves are on top of each other, demonstrating perfect 2nd-order convergence. They indicate the actual pointwise numerical error at resolution $h = 1/10$. The equivalent curves for ψ and for the Sarbach and Evans numerical methods are similar.

methods, we have also evaluated the discrete energy at every time step. With the boundary conditions $\rho\pi + \mu\pi' = 0$ and $\sigma\psi + \nu(\psi' + p\psi/r) = 0$ discussed in Appendix F we have $d\hat{E}_b/dt = 0$. With the maximally dissipative boundary condition $\rho\pi + \sigma\psi = 0$ we have $d\hat{E}/dt = \chi\pi_M\psi_M \leq 0$, and we have evolved the expected value of \hat{E} by discretising this in t using RK4. In all these cases the discrepancy between the evaluated and predicted numerical energy is of relative size 10^{-8} , essentially independent of the choice of SBP method and of the resolution, and increases linearly with t . These observations are compatible with the expectation of ac-

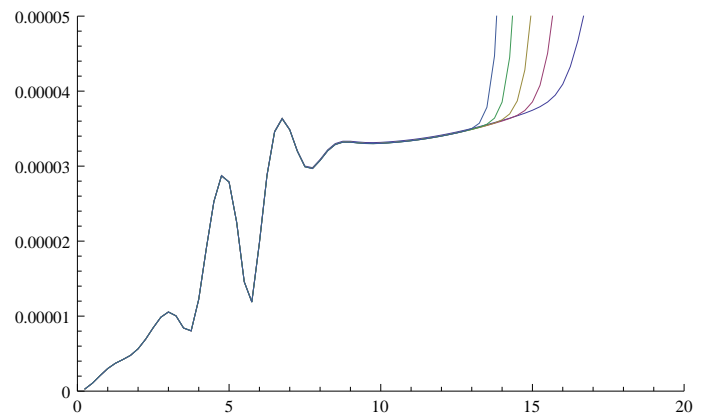


FIG. 3. 4th-order convergence in the energy norm of SBP41. We show $|e_{\pi,4}(\cdot, t; h)|$ against t , with all other details of the initial data and evolution as for the previous figure. The 5 curves are on top of each other, demonstrating perfect 4th-order convergence until $t \sim 12$, when the interaction of the tail of the Gaussian initial data with the outer boundary begins to dominate the error. The equivalent curve for ψ looks similar, and the equivalent curves for SBP42 are identical until $t \sim 12$.

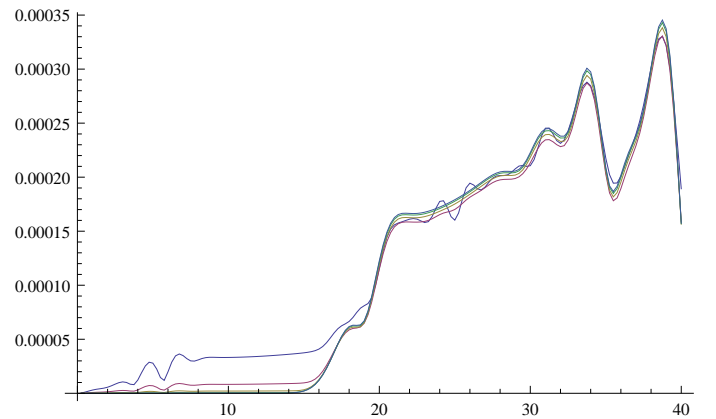


FIG. 4. 2nd-order convergence in the energy norm of SBP41 for $p = 6$, after the wave has first interacted with the boundary. We show $|e_{\pi,2}(\cdot, t; h)|$ (instead of e_4) against t , with all other details as in the previous figure. The 5 curves are on top of each other, demonstrating approximate 2nd-order convergence after $t \sim 20$, when the error generated by the interaction of the tail of the Gaussian initial data with the outer boundary dominates the error. The equivalent curve for ψ looks similar.

cumulated round-off (machine precision) error, with zero finite-differencing error.

The energy of SBP4 is not positive definite on the staggered grid for $p = 1, 2$, and so we would not expect it to be stable. However, we do not see signs of instability in our numerical experiments.

The Sarbach method behaves like SBP2 and Evans for $p \lesssim 8$, but requires a much smaller Courant factor in order to be stable for larger p : for $p = 10, 12$ and 22 , we empirically find that the Courant factor needs to be reduced to $1/8, 1/16$ and $1/800$, respectively. By con-

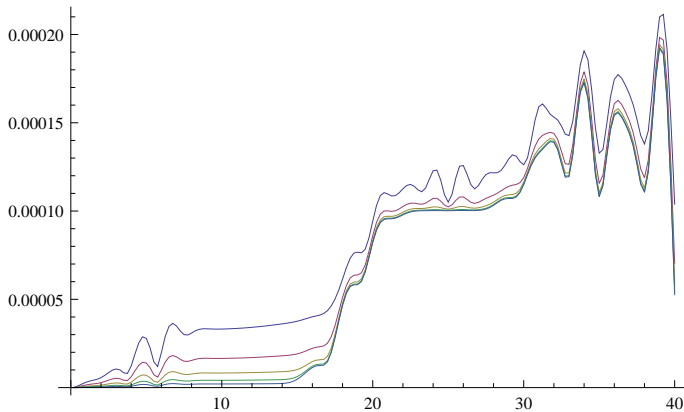


FIG. 5. 3rd-order convergence in the energy norm of SBP42 for $p = 6$, after the wave has first interacted with the boundary. We show $|e_{\pi,3}(t;h)|$ against h , with all other details as in the previous figure. The 5 curves are on top of each other, demonstrating approximate 3rd-order convergence after $t \sim 20$.

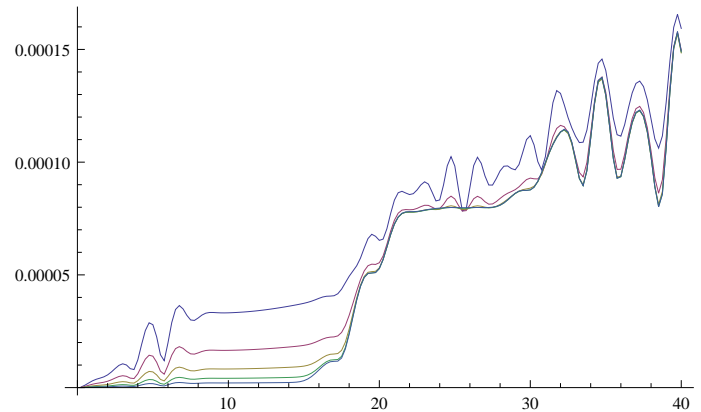


FIG. 7. 3rd-order convergence in the energy norm of SBP42 for $p = 6$, with a *derivative* boundary condition, after the wave has first interacted with the boundary. This is similar to Fig. 5, except that the boundary condition at $r = R$ is now $\pi + \pi' = 0$ instead of $\pi = 0$.

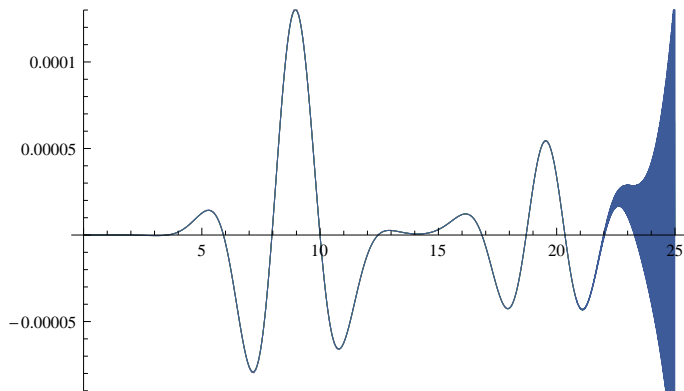


FIG. 6. 4th-order pointwise convergence of SBP42 before the wave interacts with the outer boundary. We show $e_{\pi,4}(r,t;h)$ at $t = 14.25$ against r at 5 different resolutions. The 5 curves are on top of each other, demonstrating pointwise 4-th order convergence, for $0 \leq r \lesssim 22$, which is the region not yet in contact with the outer boundary at this time. They again indicate the actual numerical error at resolution $h = 1/10$. What looks like a filled region for $r \gtrsim 22 \leq 25$ is in fact an oscillation at the grid frequency of the lowest resolution, with a smooth envelope. This is the 3rd-order error emanating from the outer boundary (and so the curves are no longer on top of each other at this resolution). $t = 14.25$ has been chosen here as the moment when the boundary error is just beginning to dominate. Compare Fig. 2, which shows the same moment of time of the evolution with SBP2, with no effect from the boundary. The equivalent figures for SBP41 and ψ look similar.

trast, all other SBP methods are stable with RK4 with a Courant factor of $1/4$ up to $p = 22$.

Finally, we have also implemented the obvious naive, non-SBP, second-order accurate finite difference method in which all derivatives are just evaluated using centred derivatives, and the p/r term is evaluated pointwise, as-

suming a staggered grid. In our notation this corresponds to defining

$$\tilde{D}\psi_i = D\psi_i + p\psi_i/r_i \quad (97)$$

on a staggered grid, with D given by (31) and ghost points at the origin. This method is unstable at the origin for all $p > 0$, with blowup occurring more rapidly for larger p , and more rapidly at higher resolution. This failure of the “standard” method (which is SBP and hence stable for $p = 0$) was of course the motivation for our work. [At the outer boundary $r = R$, we implemented “copy” (zeroth-order extrapolation) boundary conditions for this test, but we moved the outer boundary very far out so that the wave does not interact with the boundary, even numerically, before the blowup occurs. We are therefore certain that the instability of this method is due to the p/r term and not to our particular choice of outer boundary condition.]

VI. CONCLUSIONS

It is surprising that the lower-order term p/r in (1) alone can make standard finite differencing schemes unstable, and that an elaborate SBP scheme is necessary. Note however that a standard centred finite difference implementation of the one-dimensional wave equation is already SBP except possibly at the boundaries, while the equivalent naive finite differencing of (1) for $p > 0$ is not SBP even at interior points.

It seems highly unlikely to us that any scheme for (1) that is not SBP can be made stable without using numerical dissipation, for any choice of discrete boundary condition. Numerical dissipation *can* in fact stabilise the non-SBP discretisation (97), but more and more dissipation is required with increasing p , making this approach useless for even moderately large p . Again we suspect

that this will be so for any non-SBP scheme. This rules out non-SBP finite differencing schemes for large p . Furthermore, in applications where the physical growth or decay of the continuum solution is under investigation (for example, in stellar perturbation theory), the numerical method should be as little dissipative as possible.

The Evans method has been used with success previously (see [23] for a $p = 2$ application and [11] for $p \geq 2$), but we have here turned it into a complete SBP method by the appropriate modification at the outer boundary $r = R$. This modification would not have been obvious outside of an SBP framework. The Evans method and our SBP2 method work equally well for all p . The Evans method is simpler to implement, but it does not exist for odd p on a centred grid, in which case SBP2 can be used instead.

For higher accuracy, our SBP42 method should be used. It works for any p on both centred and staggered grid. (SBP41 is described here only for presentation purposes and numerical tests). It requires loading the coefficients of \tilde{D} from a file [24], but is otherwise as simple to implement as any other method, and its stencil has only 5 points (except near the origin), as narrow as possible for a 4th-order accurate method.

In hindsight we note that discrete energy conservation bounds only $r^{p/2}\pi$ and $r^{p/2}\psi$. As the maximum of $r^{-p/2}$ on the grid increases as $h^{-p/2}$ with resolution, the maximum of the numerical solution can in principle increase by the same factor, allowing it to become very much larger than the continuum solution. We find empirically that this happens in the Sarbach method with $p \gtrsim 8$, effectively leading to blowup even though a numerical energy \hat{E} is conserved, unless the Courant number is severely reduced, but that it does not happen in the other SBP methods. We have no rigorous explanation for this, but it may be connected to the fact that the local error near the origin in the Sarbach method is dominated by $O(h^2/r^2) = O(i^2)$ terms while the local error in the other methods is $O(h^2)$ uniformly in r .

The construction of our SBP4 method is designed to achieve a *uniform* in r bound on the local error (and the failure of the Sarbach method at large p seems to justify the need for this). It may be possible that a uniformly fourth-order accurate SBP method exists in which the coefficients of \tilde{D} can be given in closed form (as they are for the second-order accurate Evans method), but we have not found such a method.

To summarise our results: Until now, the only known stable numerical method for the wave equation (1) on the semi-infinite domain $0 \leq r < \infty$ was the Evans method. We have shown that it is stable because it is SBP. We have generalised it to the finite domain $0 \leq r \leq R$, and to grids both centred and staggered with respect to $r = 0$, for arbitrary p .

Going beyond 2nd-order accuracy, we have given 4th-order accurate SBP operators on this finite domain on both centred and staggered grids, and we have described a general strategy for constructing SBP operators of *ar-*

bitrary accuracy. We have proved SBP for these methods for the usual maximally dissipative boundary conditions at $r = R$, which include Dirichlet and Neumann boundary conditions, and for two families of boundary conditions involving first derivatives of π or ψ .

Our work can be seen as generalising the work of Strand on SBP operators of arbitrary accuracy from the case $p = 0$ to the case $p > 0$, motivated by applications of the wave equation in spherical rather than Cartesian coordinates.

ACKNOWLEDGMENTS

We would like to thank Olivier Sarbach for instructive conversations and comments on the manuscript, and Piotr Bizón for pointing out the application of our methods to general n . JMM was supported by ANR grant BLAN07-1_201699 “LISA Science”, and also in part by MICINN projects FIS2009-11893 and FIS2008-06078-C03-03. CG would like to thank GRCo/IAP and LUTH/Observatoire de Meudon for hospitality, and was partly supported by ANR grant 06-2-134423 “Mathematical Methods in General Relativity”. DG was supported by NSF grant PHY-0855532.

Appendix A: Rigorous treatment of ghost points at $r = 0$

We initially assume a staggered grid. Consider $\dot{\Psi}_i$ for physical grid points $i > 0$. We can write the use of ghost points explicitly as

$$\dot{\Psi}_i = h^{-1} \sum_{j>0} (D_{ij}\Pi_j + D_{i,-j}\Pi_{-j}) = h^{-1} \sum_{j>0} D_{ij}^{(+)}\Pi_j, \quad (\text{A1})$$

where

$$D_{ij}^{(+)} \equiv D_{ij} + D_{i,-j}, \quad i, j > 0. \quad (\text{A2})$$

We think of this as “folding over the ghost points”. A similar observation holds for \tilde{D} , except that as Ψ_i is odd, the equivalent of (A2) is

$$\tilde{D}_{ij}^{(+)} \equiv \tilde{D}_{ij} - \tilde{D}_{i,-j}, \quad i, j > 0. \quad (\text{A3})$$

Note that $D_{ij}^{(+)} \neq D_{ij}$ even for $i, j > 0$, thus requiring a separate symbol. (The symbol $D^{(+)}$ is a reminder of the range $i, j > 0$.) The split of $D_{ij}^{(+)}$ into D_{ij} and $D_{i,-j}$ for $i, j > 0$ is in general not unique. We do, however, have a natural prescription for this split if we assume that D_{ij} is translation-invariant, i.e. depends only on $i - j$ even at the boundary.

In order to extend D_{ij} and \tilde{D}_{ij} to negative i , we use the requirement that (28) hold at all times, or

$$\dot{\Pi}_{-i} = \dot{\Pi}_i, \quad \dot{\Psi}_{-i} = -\dot{\Psi}_i. \quad (\text{A4})$$

The first equation of (28) and the second equation of (A4) immediately give, for $i, j > 0$, that

$$D_{ij} + D_{i,-j} + D_{-ij} + D_{-i,-j} = 0. \quad (\text{A5})$$

The second equation of (28) and the first equation of (A4), after substituting (27) and using (29), give, for $i, j > 0$, that

$$(W^{-1})_{ik} (D_{kl} - D_{k,-l} - D_{-kl} + D_{-k,-l}) W_{lj} = 0, \quad (\text{A6})$$

and hence

$$D_{ij} - D_{i,-j} - D_{-ij} + D_{-i,-j} = 0. \quad (\text{A7})$$

Taking the sum and difference of (A5) and (A7), we obtain (30).

Finally, we have, for $i, j > 0$, that

$$\begin{aligned} \tilde{D}_{ij}^{(+)} &= \sum_{k,l>0} -(W^{-1})_{ik} (D_{lk} - D_{-lk}) \tilde{W}_{lj} \\ &= \sum_{k,l>0} -(W^{-1})_{ik} (D_{lk} + D_{l,-k}) \tilde{W}_{lj} \\ &= \sum_{k,l>0} -(W^{-1})_{ik} (D^{(+t)})_{kl} \tilde{W}_{lj}, \end{aligned} \quad (\text{A8})$$

and so (25) holds for the operators $D^{(+)}$ and $\tilde{D}^{(+)}$ with ghost points folded in if and only if it holds for the extended operators D and \tilde{D} . This confirms that the introduction of ghost points is just a matter of notation (or coding).

A similar argument goes through on a centred grid, with the point $i = 0$ “split” between the domains $r \geq 0$ and $r \leq 0$. Here we note only that when removing the ghost points, the discrete energy on a centred grid is

$$\begin{aligned} \hat{E} &= \frac{h^{p+1}}{4} (W_{00} \Pi_0^2 + \tilde{W}_{00} \Psi_0^2) \\ &+ \frac{h^{p+1}}{2} \sum_{i,j=1}^M (W_{ij} \Pi_i \Pi_j + \tilde{W}_{ij} \Psi_i \Psi_j). \end{aligned} \quad (\text{A9})$$

(Note the $1/4$.)

Appendix B: Solution of the recurrence relations

In the $N = 1$ case, the recurrence relation Eq. (51) for the w_i is solved as follows. To work with a bounded quantity, we define the new variable \bar{w}_i as

$$w_i = i^p \bar{w}_i. \quad (\text{B1})$$

(Therefore $\bar{w}_{-i} = -\bar{w}_i$ for odd p , while $w_i > 0$.) It obeys the linear recurrence relation

$$\bar{w}_i = \frac{2(p+1)}{i} \left(1 - \frac{1}{i}\right)^p \bar{w}_{i-1} + \left(1 - \frac{2}{i}\right)^{p+1} \bar{w}_{i-2}. \quad (\text{B2})$$

Trying asymptotic solutions of the form

$$\bar{w}_i = \rho^i \sum_{m=0}^{\infty} C_m i^{k-m} \quad (\text{B3})$$

for constants ρ and k shows that the two linearly independent solutions have $\rho = \pm 1$ and are (fixing a constant overall factor, and assuming $i > 0$)

$$\bar{w}_i^{(+)} = 1 + \frac{p(p^2 - 1)}{12i^2} + O(i^{-4}), \quad (\text{B4})$$

$$\bar{w}_i^{(-)} = (-1)^i i^{-2(p+1)} \left(1 - \frac{(p+1)(p+2)(p+3)}{12i^2} + O(i^{-4})\right). \quad (\text{B5})$$

The first one is asymptotically constant, and the second is an oscillating decaying solution. The general asymptotic solution is an arbitrary linear combination of those, and hence it is also asymptotically constant. [The asymptotically constant mode (B4) for given p is a finite polynomial in i^{-2} of (the integer part of) $1+p/2$ terms. For example, restricting to $i > 0$, for $p = 1$ we have $\bar{w}_i^{(+)} = 1$ and for $p = 2$ we have $\bar{w}_i^{(+)} = 1 + 1/(2i^2)$.]

From these results we can infer the asymptotic behaviour of the $\delta_{\alpha i}$. If \bar{w}_i tends to a constant $\bar{w}_{\infty} \neq 0$ then we have

$$\delta_{0i} = \frac{p(1-p)}{2} + O(i^{-2}), \quad (\text{B6})$$

$$\delta_{1i} = \frac{p}{2} + O(i^{-2}). \quad (\text{B7})$$

Only in the case where $\bar{w}_{\infty} = 0$ and only the oscillating mode is present is there a divergence in δ_1 , namely

$$\delta_{0i} = 2i^2 + \frac{(p+2)(p+3)}{2} + O(i^{-2}), \quad (\text{B8})$$

$$\delta_{1i} = \frac{p+2}{2} + O(i^{-2}). \quad (\text{B9})$$

However, with our initial data $w_{-1/2} = w_{1/2}$ on the staggered grid or $w_1 = (1+p)w_0$ on the centred grid, the constant solution is present, and hence the sequence $\delta_{\alpha i}$ converges as $i \rightarrow \infty$, and is therefore bounded. Furthermore, the upper bound of its absolute value is close to the asymptotic value, as we show in Fig. 8.

Finally, we adjust the arbitrary overall factor such that $\lim_{i \rightarrow \infty} \bar{w}_i = 1$. On the centred grid we need

$$w_0 = \frac{p!}{2^p} \quad (\text{B10})$$

for any value of p . \bar{w}_i for $i > 0$ is then actually given by the asymptotically constant polynomial (B4). (For even p , this is true for all i , but not for $i = 0$ with odd p , where the special form of the accuracy condition at the centre needs to be used.)

On the staggered grid we need for even p

$$\bar{w}_{1/2} = \frac{[(p+1)!!]^2}{p+1}, \quad (\text{B11})$$

which also leads to the polynomials (B4). However for odd p the symmetry condition at the centre is incompatible with having only the asymptotically constant mode, and we need a contribution from the oscillating mode (B5). For $\lim_{i \rightarrow \infty} \bar{w}_i = 1$ we now need

$$\bar{w}_{1/2} = \frac{2[(p+1)!!]^2}{\pi(p+1)}. \quad (\text{B12})$$

The method for solving the recurrence relation in the $N = 2$ case is similar. With the equivalent of (B1) and (B3) for v_i , the fourth-order linear recurrence for \bar{v}_i has four independent asymptotic solutions with

$$\rho = 1, \quad -1, \quad 4 + \sqrt{15}, \quad 4 - \sqrt{15}, \quad (\text{B13})$$

all with $k = 0$. The linearity of the recurrence relation implies that the general solution \bar{v}_i is a linear combination of the four corresponding modes $\bar{v}_i^{(\rho)}$. It is possible to show that if the linear combination contains any contribution of the growing or oscillating modes then the δ_α are not bounded. Hence we must find a solution which only contains the asymptotically constant and the decaying modes. The freedom in u_1 , $v_{1/2}$ and $v_{3/2}$ on the staggered grid, and in $u_{3/2}$, $u_{5/2}$ and v_1 on the centred grid allows us precisely to cancel simultaneously the growing mode and the oscillating non-decaying mode and fix an overall constant factor. To do that we proceed as follows.

We first compute three arbitrary solutions of the recurrence up to some high value of i , say 1000. For example, on the staggered grid we can set each of u_1 , $v_{1/2}$ and $v_{3/2}$ to 1 and the other two to 0. The three solutions are dominated by the growing mode, and reach very high values, of order $(4 + \sqrt{15})^{1000} \sim 10^{896}$. We have detected extreme sensitivity of the solution to the initial conditions, roughly losing one decimal digit of precision per iteration, and hence the recurrence is solved with exact rational arithmetic, using *Mathematica*.

Then we compute the asymptotic form of the modes, up to order $O(i^{-8})$. For instance for the asymptotically constant mode we have

$$\begin{aligned} \bar{v}_i^{(1)} = 1 + & \frac{(2p-1)(p-1)p(p+1)(p+3)}{60i^4} \\ & + \frac{(2p-3)(p-3)(p-2)(p-1)p(p+1)(p+3)}{504i^6} \\ & + O(i^{-8}). \end{aligned} \quad (\text{B14})$$

[for $p = 2$ this is simply $1 + 3/(2i^4) + O(i^{-8})$.] However, in contrast to the $N = 1$ case, these are finite polynomials only for odd p , but not for even p . For $i \sim 1000$ this expression will give results correct up to relative errors smaller than 10^{-18} for $p \leq 10$. We take three such values of i and construct a linear system to find which linear combination of our three solutions gives that mode $\bar{v}_i^{(1)}$.

For such high values of i we can neglect the contribution of the decaying mode. In this way we determine the values of \bar{v}_i up to $i = 1000$. For larger i , and $p \leq 10$, the asymptotic series are accurate to 16 digits. In our experiments below we shall use up to $p = 22$, for which values up to $i = 2000$ must be computed to use the given asymptotic expansions with relative errors below double precision. Note that we do not know if these series are convergent.

From v_i we can compute w_i . This gives the following asymptotic behaviour for \bar{w}_i ,

$$\begin{aligned} \bar{w}_i = 1 + & \frac{(2p+1)(p+1)p(p-1)(p-3)}{60i^4} \\ & + \frac{(2p-1)(p-5)(p-3)(p-2)(p-1)p(p+1)}{504i^6} \\ & + O(i^{-8}). \end{aligned} \quad (\text{B15})$$

For $i \geq 9/2$ on the staggered grid and $i \geq 6$ on the centred grid the δ can be computed from v_i and w_i as follows,

$$\delta_{0i} = i^5 \frac{v_{i-2} - 8v_{i-1} + 8v_{i+1} - v_{i+2}}{12w_i} - p i^4, \quad (\text{B16})$$

$$\delta_{1i} = i^2 \frac{v_{i-2} - v_{i-1} - v_{i+1} + v_{i+2}}{9w_i}, \quad (\text{B17})$$

$$\delta_{2i} = i \frac{2v_{i-2} - v_{i-1} + v_{i+1} - 2v_{i+2}}{36w_i}. \quad (\text{B18})$$

The previous expansions imply that the δ are bounded and have finite limits:

$$\delta_{0i} = -p(p-1)^2 + O(i^{-2}) \quad (\text{B19})$$

$$\delta_{1i} = \frac{p(p-1)}{3} + O(i^{-2}), \quad (\text{B20})$$

$$\delta_{2i} = -\frac{p}{6} + O(i^{-2}). \quad (\text{B21})$$

The limit value of δ_0 is cubic in p . That means that δ_0 is very large for large values of p . Comparing with $N = 1$ it is plausible that δ_0 has an asymptotic limit which grows like p^{N+1} .

We provide in our webpage [24] data files with double-precision results for \bar{v} , \bar{w} and the δ for $1 \leq p \leq 22$ and $i \leq 2000$. Formulas (B14) and (B15) can be used to compute \bar{v} and \bar{w} for these p and $i > 2000$ to 16 digits.

We find that for $p = 1$ and $p = 2$ (the wave equation in cylindrical and spherical symmetry), on the staggered grid, $v_{1/2} < 0$, so that \tilde{W} is then not positive definite. This problem is absent for $p \geq 3$, or on the centred grid. It is possible that allowing for u_i other than u_1 to be nonzero this could be fixed, but we have not tried this.

Appendix C: The Evans method

Here we review the method of Evans [16] in the notation of our paper and present a boundary treatment that makes it SBP. The continuum identity

$$\psi' + \frac{p}{r}\psi = (p+1) \frac{d(r^p \psi)}{d(r^{p+1})} \quad (\text{C1})$$

suggests the difference operator \tilde{D} given by

$$h^{-1}(\tilde{D}\Psi)_i = (p+1) \frac{r_{i+1}^p \Psi_{i+1} - r_{i-1}^p \Psi_{i-1}}{r_{i+1}^{p+1} - r_{i-1}^{p+1}}. \quad (\text{C2})$$

We combine it with the usual second-order accurate 3-point symmetric difference operator (31). Comparing (49) with (C2) we see that the Evans method is then SBP with

$$v_i = i^p, \quad (\text{C3})$$

$$w_i = \frac{(i+1)^{p+1} - (i-1)^{p+1}}{2(p+1)}. \quad (\text{C4})$$

We note that these are well defined for all i including $i = 0$. Indeed, the accuracy conditions at the origin (35) for a method with diagonal energy (48) reduce to $v_1 = (1+p)w_0$, which is easily seen to hold for the ansatz (C3,C4) for even p . Note that the Evans method does not work for odd p (the wave equation in even space dimensions) on a staggered grid, as then $w_0 = 0$. The plots in the right half of Fig. (8) show that this method is second-order accurate uniformly in r , like our method SBP2.

To our knowledge, no SBP treatment of the outer boundary for the SBP method has been given. However, our general method of Sec. IV immediately gives us a prescription, namely (81,80).

The identity (C1) seems at first sight to suggest a generalization of the Evans method to accuracy order $2N$, discretizing $d/dr + p/r$ as

$$(p+1) \frac{D(r^p \Psi)}{D(r^{p+1})}, \quad (\text{C5})$$

where D is some discretization of d/dr of accuracy order $2N$. If we take the norms

$$v_i = i^p, \quad w_i = \frac{1}{p+1} D(i^{p+1}), \quad (\text{C6})$$

then (C5) also obeys the SBP property. However, for the minimal-width centred stencils D of order larger than 2 this does not work. To see this we differentiate $\psi(r) = ar + br^3$ using the operators D of accuracy $N = 1$ and $N = 2$. The discretization errors are, respectively,

$$b(p+3)(2p+1)h^2 + O(h^3), \quad (\text{C7})$$

$$-\frac{2b(p+3)p(p-1)(2p-1)}{15} \frac{h^4}{r^2} + O(h^5). \quad (\text{C8})$$

In the latter case we see an error of the form h^4/r^2 , which becomes h^2 near the centre.

We have not been able to generalize the Evans method to avoid this type of singular error term.

Appendix D: The Sarbach method

Here we review the method of Sarbach [17, 18] in the notation of our paper. The continuum identity

$$\psi' + \frac{p}{r}\psi = \frac{(r^p \psi)'}{r^p} \quad (\text{D1})$$

suggests the finite differencing operator

$$(\tilde{D}\Psi)_i = \frac{(i+1)^p \Psi_{i+1} - (i-1)^p \Psi_{i-1}}{2i^p}. \quad (\text{D2})$$

In [17, 18] this is used on the interior points of a centred grid. At the symmetry boundary

$$(\tilde{D}\Psi)_0 = (p+1)\Psi_0, \quad (\text{D3})$$

and at the outer boundary

$$(\tilde{D}\Psi)_M = \frac{M^p \Psi_M - (M-1)^p \Psi_{M-1}}{M^p}. \quad (\text{D4})$$

This fits into our general approach with

$$v_i = w_i = i^p \quad \text{for } i \neq 0, \quad (\text{D5})$$

$w_0 = 2/(1+p)$, and the outer boundary treatment (81,80), and hence is SBP.

It also appears to be second-order accurate, but it is not uniformly so, in contrast to the methods derived here. As an example, for $\psi = r$ (i.e. generic behaviour at the origin) and $p = 2$, the local error of the finite differencing operator $h^{-1}\tilde{D}$ is exactly $h^2/r^2 = 1/i^2$. (For higher $p > 0$, terms up to $(h/r)^p$ also appear.) This does not go to zero with h at fixed i . However, for $p \neq 2, 3$ the method converges with h^2 in the energy norm [25].

Appendix E: Continuum boundary conditions involving derivatives

Consider the class of boundary conditions of the form

$$\rho\pi + \sigma\psi + \mu\pi' + \nu\left(\psi' + \frac{p}{r}\psi\right) = 0, \quad r = R \quad (\text{E1})$$

or equivalently

$$\rho\pi + \sigma\psi + \mu\dot{\psi} + \nu\dot{\pi} = 0, \quad r = R \quad (\text{E2})$$

for ρ, σ, μ, ν not all vanishing at once. To fix an overall sign, we also assume that at least one of them is positive. We now use an energy argument to show that these boundary conditions give rise to a stable initial-boundary value problem if $\rho, \sigma, \mu, \nu \geq 0$ with $\rho\mu + \sigma\nu > 0$. [The maximally dissipative special case $\mu = \nu = 0$ with $\rho\sigma \geq 0$ is also stable based on the energy E defined in (2)].

We consider the energy

$$E_b \equiv E + \frac{R^p}{2s} (\mu\psi + \nu\pi)_{r=R}^2, \quad (\text{E3})$$

where E is given by (2), E_b stands for E modified by a boundary term, and s is

$$s \equiv \rho\mu + \sigma\nu. \quad (\text{E4})$$

Its time derivative is

$$\begin{aligned}\frac{dE_b}{dt} &= R^p \left[\pi\psi + \frac{1}{s}(\mu\psi + \nu\pi) \left(\mu\dot{\psi} + \nu\dot{\pi} \right) \right]_{r=R} \\ &= R^p \left[\pi\psi - \frac{1}{s}(\mu\psi + \nu\pi) (\rho\pi + \sigma\psi) \right]_{r=R} \\ &= -\frac{R^p}{s}(\mu\sigma\psi^2 + \nu\rho\pi^2)_{r=R},\end{aligned}\quad (\text{E5})$$

The necessary and sufficient conditions for E_b to be positive definite and its time derivative to be non-positive are

$$\rho \geq 0, \quad \sigma \geq 0, \quad \mu \geq 0, \quad \nu \geq 0. \quad (\text{E6})$$

We have $dE_b/dt = 0$ if $\mu\sigma = \rho\pi = 0$, and $dE_b/dt < 0$ otherwise. However, the limiting case $\rho\mu = \sigma\nu = 0$ is not allowed because it would give $s = 0$, except for the maximally dissipative sub-case $\mu = \nu = 0$, where E and dE/dt are given by (2) and (3) instead of (E3) and (E5).

Appendix F: Numerical boundary conditions involving derivatives

We define the modified numerical energy

$$\hat{E}_b = \hat{E} + \frac{\chi h^p M^p}{2s} (\mu\Psi_M + \nu\Pi_M)^2, \quad (\text{F1})$$

where χ parameterises finite differencing error in the boundary term, as defined by (26). We find

$$\begin{aligned}\frac{d\hat{E}_b}{dt} &= \chi h^p M^p \left[\Pi_M \dot{\Psi}_M \right. \\ &\quad \left. + \frac{1}{s} (\mu\dot{\Psi}_M + \nu\dot{\Pi}_M) \left(\mu\dot{\Psi}_M + \nu\dot{\Pi}_M \right) \right],\end{aligned}\quad (\text{F2})$$

so if the numerical boundary could be chosen to be

$$\rho\pi_M + \sigma\psi_M + \mu\dot{\psi}_M + \nu\dot{\pi}_M = 0, \quad (\text{F3})$$

the argument could be completed as in the continuum case. However, in the notation of Appendix G, $\dot{u} = \mathcal{P}\mathcal{D}u$ and not $\mathcal{D}u$. We have not been able to find an ansatz for \mathcal{L} and \hat{E}_b such that $d\hat{E}_b/dt \leq 0$.

Consider however the two subclasses of boundary conditions where $dE_b/dt = 0$ in the continuum. Consider first the case $\sigma = \nu = 0$ with $\rho\mu > 0$. Then (F2) reduces to

$$\begin{aligned}\frac{d\hat{E}_b}{dt} &= \chi h^p M^p \left(\Pi_M \dot{\Psi}_M + \frac{\mu}{\rho} \Psi_M \dot{\Psi}_M \right) \\ &= \chi h^p M^p \left(\Pi_M \dot{\Psi}_M + \frac{\mu}{\rho} \Psi_M h^{-1} (D\Pi)_M \right) \\ &= 0,\end{aligned}\quad (\text{F4})$$

where the second equality holds because in this special case the boundary condition is independent of Ψ so that

\mathcal{P} only acts on Π , and the last equality holds if we implement $\mathcal{L}u = 0$ as

$$\rho\Pi_M + \mu h^{-1} (D\Pi)_M = 0. \quad (\text{F5})$$

The case $\rho = \mu = 0$ with $\nu\sigma > 0$ works the same way, with the roles of Π and Ψ interchanged.

Appendix G: The projection method for imposing boundary conditions

For completeness, this Appendix summarises relevant methods from [19]. Suppose a first-order in space and time system of PDEs in one spatial dimension has been discretised in space as

$$\dot{u} = \mathcal{D}u \quad (\text{G1})$$

Note that the vector u in general ranges over multiple variables (for example π and ψ) as well as grid points (for example i), and we use calligraphic letters such as \mathcal{D} for operators on this vector space.

Suppose this system has a discrete energy

$$\hat{E} \equiv \frac{1}{2} u^t \mathcal{W} u \quad (\text{G2})$$

and obeys the SBP property that

$$\mathcal{B} \equiv \frac{1}{2} (\mathcal{W}\mathcal{D} + \mathcal{D}^t\mathcal{W}) \quad (\text{G3})$$

is a boundary operator. Then

$$\frac{d\hat{E}}{dt} = u^t \mathcal{B} u \quad (\text{G4})$$

is a boundary term.

We want to impose one or several homogenous linear boundary conditions that we write as

$$\mathcal{L}u = 0. \quad (\text{G5})$$

In matrix notation where u is a column vector, \mathcal{L} is a matrix that has one row for each boundary condition.

We define the inner product

$$(u, v) \equiv u^t \mathcal{W} v. \quad (\text{G6})$$

In this notation we can write

$$\hat{E} = \frac{1}{2} (u, u), \quad \frac{d\hat{E}}{dt} = (u, \mathcal{D}u). \quad (\text{G7})$$

The adjoint with respect to this inner product is defined by

$$(\mathcal{A}u, v) \equiv (u, \mathcal{A}^\dagger v), \quad (\text{G8})$$

and is therefore given by

$$\mathcal{A}^\dagger = \mathcal{W}^{-1} \mathcal{A}^t \mathcal{W}. \quad (\text{G9})$$

The operator

$$\mathcal{P} \equiv 1 - \mathcal{W}^{-1} \mathcal{L}^t (\mathcal{L} \mathcal{W}^{-1} \mathcal{L}^t)^{-1} \mathcal{L} \quad (\text{G10})$$

clearly obeys

$$\mathcal{P}^2 = \mathcal{P}, \quad \mathcal{L} \mathcal{P} = 0, \quad \mathcal{P}^\dagger = \mathcal{P}, \quad (\text{G11})$$

and so is a self-adjoint projection operator into the space of grid functions that obey the boundary conditions. If we now use the semi-discrete evolution equation

$$\dot{u} = \mathcal{P} \mathcal{D} u \quad (\text{G12})$$

instead of (G1), we have $\mathcal{L} \dot{u} = 0$ exactly, and hence $\mathcal{L} u = 0$ and therefore $\mathcal{P} u = u$ at all times if it holds initially. Then we have

$$\frac{d\hat{E}}{dt} = (u, \mathcal{P} \mathcal{D} u) = (\mathcal{P} u, \mathcal{D} u) = (u, \mathcal{D} u) \quad (\text{G13})$$

as before and so both the discrete energy bound and the desired boundary conditions hold.

-
- [1] B. Gustafsson, H.-O. Kreiss and J. Olinger, *Time-dependent Problems and Difference Methods*, Wiley, New York 1995.
- [2] G. Calabrese, L. Lehner, O. Reula, O. Sarbach and M. Tiglio, Summation by parts and dissipation for domains with excised regions, *Class. Quant. Grav.* **21**, 5735 (2004).
- [3] L. Lehner, D. Neilsen, O. Reula and M. Tiglio, The discrete energy method in numerical relativity: Towards long-term stability, *Class. Quant. Grav.* **21** 5819 (2004).
- [4] L. Lehner, O. Reula and M. Tiglio, Multi-block simulations in general relativity: high order discretizations, numerical stability, and applications, *Class. Quant. Grav.* **22**, 5283 (2005).
- [5] B. Strand, Summation by parts for finite difference approximations for d/dx , *J. Comp. Phys.* **110**, 47-67 (1994).
- [6] P. Diener, E. N. Dorband, E. Schnetter and M. Tiglio, New, efficient, and accurate high order derivative and dissipation operators satisfying summation by parts, and applications in three-dimensional multi-block evolutions, *J. Sci. Comput.* **32**, 109 (2007).
- [7] M. Birukou, V. Husain, G. Kunstatter, E. Vaz, and M. Olivier, Spherically symmetric scalar field collapse in any dimension, *Phys. Rev. D* **65**, 104036 (2002).
- [8] E. Sorkin and Y. Oren, On Choptuik's scaling in higher dimensions, *Phys. Rev. D* **71**, 124005 (2005).
- [9] M. W. Choptuik, E. W. Hirschmann, S. L. Liebling and F. Pretorius, Critical collapse of a complex scalar field with angular momentum, *Phys. Rev. Lett.* **93**, 131101 (2004).
- [10] C. Gundlach and J. M. Martín-García, Critical gravitational collapse of a perfect fluid: nonspherical perturbations, *Phys. Rev. D* **61**, 084024 (2000).
- [11] J. M. Martín-García and C. Gundlach, All nonspherical perturbations of the Choptuik spacetime decay, *Phys. Rev. D* **59**, 064031 (1999).
- [12] L. Villain and S. Bonazzola, Inertial modes in slowly rotating stars: an evolutionary description, *Phys. Rev. D* **66**, 123001 (2002).
- [13] W. Tscharnuter and K.-H. Winkler, A method for computing self-gravitating gas flows with radiation, *Computer Phys. Comm.* **18**, 171 (1979).
- [14] F. Rincon and M. Rieutord, Oscillations of magnetic stars: I. Axisymmetric shear Alfvén modes of a spherical shell in a dipolar magnetic field, *Astron. and Astrophys.* **398**, 663 (2003); **427**, 279 (2004).
- [15] D. J. Ivers and C. G. Phillips, Scalar and vector spherical harmonic spectral equations of rotating magnetohydrodynamics, *Geophys. J. Int.* **175**, 955 (2008).
- [16] C. Evans, PhD thesis, University of Texas at Austin, 1984; C. Evans, in *Dynamical Spacetimes and Numerical Relativity*, ed. J. Centrella, Cambridge University Press, Cambridge 1986.
- [17] G. Calabrese and D. Neilsen, Spherical excision for moving black holes and summation by parts for axisymmetric systems, *Phys. Rev. D* **69**, 044020 (2004).
- [18] D. Neilsen, L. Lehner, O. Sarbach and M. Tiglio, in *Analytical and Numerical Approaches to Mathematical Relativity* Lecture Notes in Physics, Volume 692, 223-249, Springer, Berlin 2006.
- [19] P. Olsson, Summation by parts, projections, and stability I, *Mathematics of Computation* **64**, 1035-1065 (1995).
- [20] M. Svärd and J. Nordström, On the order of accuracy for difference approximations of initial-boundary value problems, *J. Comp. Phys.* **218**, 333 (2006).
- [21] B. Gustafsson, The convergence rate for difference approximations to mixed initial boundary value problems, *Math. Comp.* **29**, 396 (1975).
- [22] B. Gustafsson, The convergence rate for difference approximations to general mixed initial boundary value problems, *SIAM J. Numer. Anal.* **18**, 179 (1981).
- [23] E. P. Honda and M. W. Choptuik, Fine structure of oscillons in the spherically symmetric ϕ^4 Klein-Gordon model, *Phys. Rev. D* **65**, 084037 (2002).
- [24] <http://www.soton.ac.uk/~cjpg/lwaveSBP/>. Coefficients for higher values of p are available from the authors on request.
- [25] O. Sarbach, private communication.

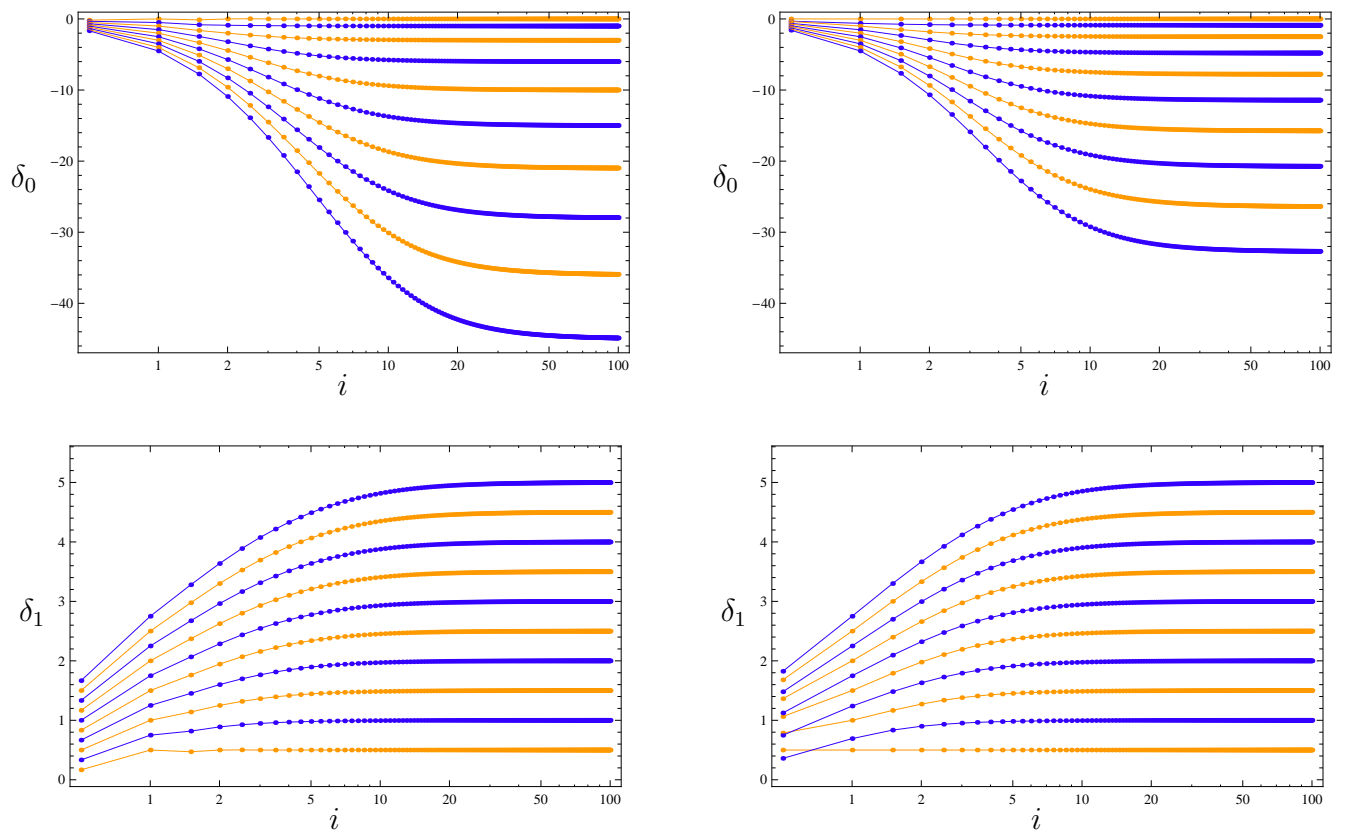


FIG. 8. Values of δ_0 and δ_1 for our second-order accurate ($N = 1$) methods, for $p = 1, \dots, 10$. SBP2 is in the left column and Evans in the right column. The staggered grids (half-integer i) and centred grids (integer i) are shown on the same plot. In all cases increasing values of p correspond to increasing $|\delta_i|$, with even values of p shown in blue (dark) and odd values in orange (light). Note that the Evans method does not exist for odd p on the centred grid, and the corresponding dots are absent. We see a rapid convergence towards the respective asymptotic values (B6) and (B7) for SBP2, and $\delta_0 \rightarrow (p+2)p(1-p)/3/(p+1)$ and $\delta_1 \rightarrow p/2$ for the Evans method. Note that the i axis is logarithmic.

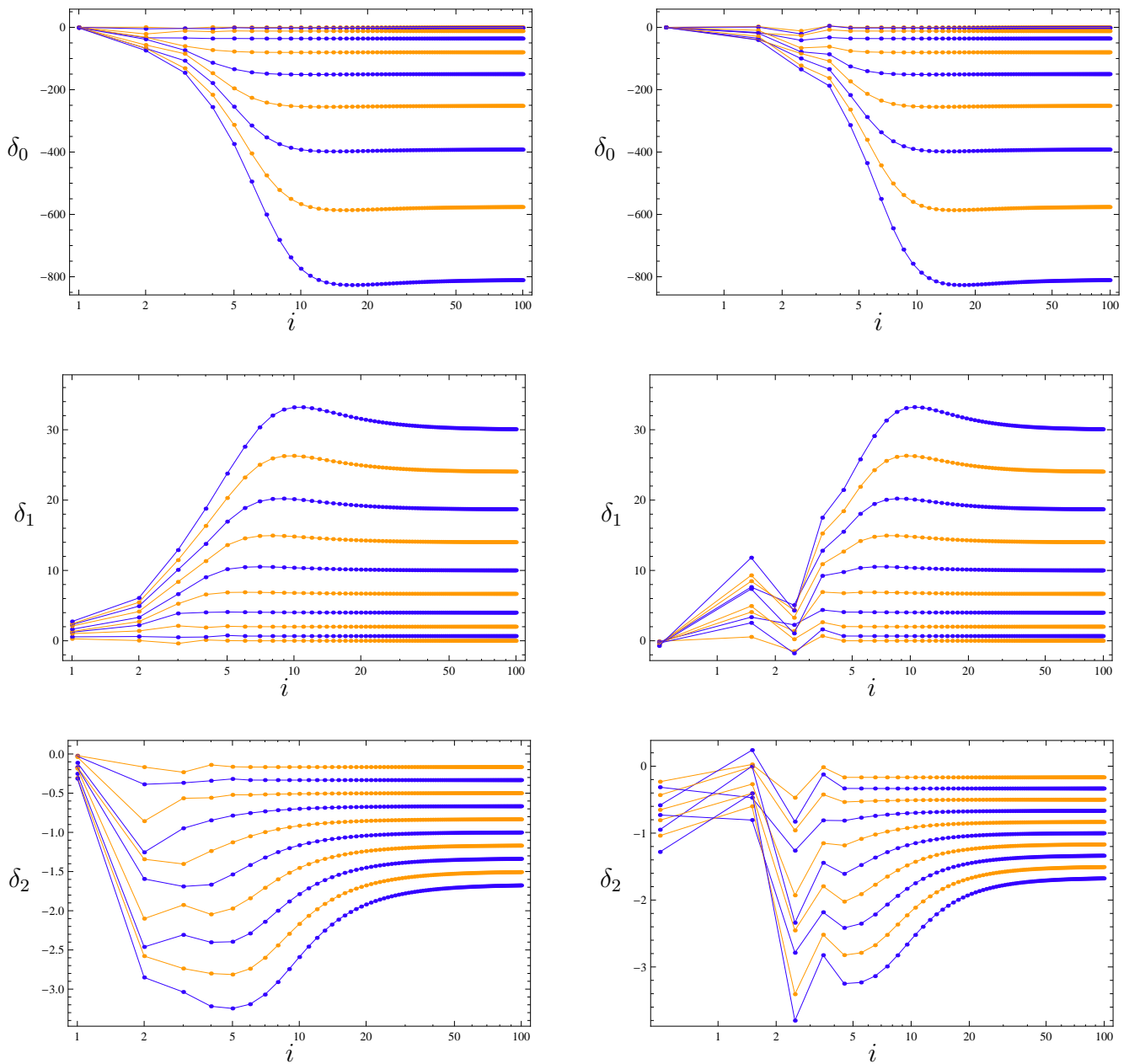


FIG. 9. Values of δ_0 , δ_1 and δ_2 for SBP4 on the centred grid (left column) and on the staggered grid (right column), with $p = 1, \dots, 10$. In all cases increasing values of p correspond to lines further from the axis $\delta_i = 0$, with even values of p shown in blue (dark) and odd values in orange (light). Again, we see a rapid convergence towards their respective asymptotic values (B19–B21). The fact that u_1 (for the staggered grid) and $u_{3/2}$ or $u_{5/2}$ (for the centred grid) appear explicitly in the recurrence for a few low i points, but not beyond, produces some irregular behaviour at those points.